The Plant Journal (2006) **47**, 174–195 doi: 10.1111/j.1365-313X.2006.02783.x

Differential display proteomic analysis of *Picea meyeri* pollen germination and pollen-tube growth after inhibition of actin polymerization by latrunculin B

Yanmei Chen[1,2], Tong Chen[1,2], Shihua Shen[1], Maozhong Zheng[1,2], Yiming Guo[1], Jinxing Lin[1,*], František Baluška[3,4] and Jozef Šamaj[3,5]

[1]*Key Laboratory of Photosynthesis and Molecular Environment Physiology, Institute of Botany, Chinese Academy of Sciences, Beijing 100093, China,*

[2]*Graduate School, Chinese Academy of Sciences, Beijing 100039, China,*

[3]*Institute of Cellular and Molecular Botany, University of Bonn, Kirschallee 1, D-53115 Bonn, Germany,*

[4]*Institute of Botany, Slovak Academy of Sciences, Dubravska 14, SK-84223, Bratislava, Slovak Republic, and*

[5]*Institute of Plant Genetics and Biotechnology, Slovak Academy of Sciences, Akademicka 2, SK-95007, Nitra, Slovak Republic*

Received 22 December 2005; revised 27 February 2006; accepted 28 February 2006.
*For correspondence (fax +86 10 62590833; e-mail linjx@ibcas.ac.cn).

Summary

To investigate roles of the actin cytoskeleton in growth of the pollen tube of *Picea meyeri*, we used the actin polymerization inhibitor latrunculin B (LATB) under quantitatively controlled conditions. At low concentrations, LATB inhibited polymerization of the actin cytoskeleton in the growing pollen tube, which rapidly inhibited tip growth. The proteomic approach was used to analyse protein expression-profile changes during pollen germination and subsequent pollen-tube development with disturbed organization of the actin cytoskeleton. Two-dimensional electrophoresis and staining with Coomassie Brilliant Blue revealed nearly 600 protein spots. A total of 84 of these were differentially displayed at different hours with varying doses of LATB, and 53 upregulated or downregulated proteins were identified by mass spectrometry. These proteins were grouped into distinct functional categories including signalling, actin cytoskeleton organization, cell expansion and carbohydrate metabolism. Moreover, actin disruption affected the morphology of Golgi stacks, mitochondria and amyloplasts, along with a differential expression of proteins involved in their functions. These findings provide new insights into the multifaceted mechanism of actin cytoskeleton functions and its interaction with signalling, cell-expansion machinery and energy-providing pathways.

Keywords: actin cytoskeleton, tip growth, proteomics, mass spectrometry, *Picea meyeri*, pollen tube.

Abbreviations. LATB, latrunculin B; PMF, peptide mass fingerprint; MALDI-TOF, matrix-assisted laser desorption/ionization time-of-flight; ASB 14, amidosulfobetaine 14; CHAPS, 3-[(3-cholamidoproply)dimethyl-ammonio]-1-propanesulfonic acid; SB 3-10, *N*-decyl-*N*,*N*-dimethyl-3-ammonio-1-propane sulfonate.

Introduction

The pollen tube is a significant tip-growing system in sexual reproduction because it delivers the sperm to the ovule. This process is highly dependent on the actin cytoskeleton. During tip growth, the actin cytoskeleton allows for vigorous cytoplasmic streaming, which moves organelles around the tube and brings the vesicles to the tip, where they fuse to produce a new cell wall and plasma membrane thus elongating the tube (Lancelle and Hepler, 1992; Vidali *et al.*, 2001). Additionally, actin is essential for endocytosis and vesicular recycling via secretory endosomes (Murphy *et al.*, 2005; Šamaj *et al.*, 2004, 2005). The actin cytoskeleton also helps to establish and maintain cell polarity, and is therefore a major target for investigating signalling cascades in pollen development and responses to different signals in higher plants (Franklin-Tong, 1999; Staiger, 2000; Volkmann and Baluška, 1999).

Latrunculin B is a macrolide toxin purified from *Latrunculia magnifica*, a Red Sea sponge, which is capable of inhibiting actin cytoskeleton polymerization both *in vitro* and *in vivo* (Spector *et al.*, 1983). LATB forms 1:1 complexes with actin monomers, thereby reducing the amount of F-actin detectable by immunocytochemistry (Coué *et al.*, 1987). In contrast to another actin inhibitor, cytochalasin D, low concentrations of LATB are sufficient to disrupt the actin cytoskeleton in living cells (Gibbon *et al.*, 1999). Furthermore, at the biochemical level, LATB has a well understood and simple mode of action resulting in a complete shift from F-actin to G-actin (Walter *et al.*, 2000). In recent years, LATB has been widely used to investigate the function of actin in a range of organisms, including gymnosperms, and monocotyledonous and dicotyledonous plants (Baluška *et al.*, 2001; Justus *et al.*, 2004; Šamaj *et al.*, 2002). Previous investigations revealed that pollen-tube growth is an actin-dependent process requiring dynamic reorganization of the actin cytoskeleton (Justus *et al.*, 2004; Lazzaro, 1998). In contrast to the vast number of morphological studies that have investigated pollen germination and tube growth, few protein-expression patterns in pollen tubes have been characterized. Pollen tubes in gymnosperms differ greatly from those of angiosperms in their slower growth rates (Lazzaro, 1998; Pendleton *et al.*, 2003); extended periods of growth (Lazzaro, 1998); and delayed gametogenesis (Parton *et al.*, 2001; Pierson *et al.*, 1996). Furthermore, cytoskeleton and vesicular trafficking differ between the two groups (Justus *et al.*, 2004; Wang *et al.*, 2005). These differences may indicate that the pollen tubes in gymnosperms and angiosperms develop and elongate via different mechanisms. Because many proteins associated with the actin cytoskeleton are probably involved in the signalling pathways that control pollen development (Gibbon *et al.*, 1999; Vidali *et al.*, 2001), a proteomic investigation could help elucidate the signalling cascades that modulate pollen-tube growth and actin dynamics at the protein level.

Proteomic analysis is an emerging technology that can overcome some of the shortcomings of genomic approaches. Combining the high resolution of two-dimensional electrophoresis (2-DE) and sensitive mass spectrometry, proteomic analysis is a powerful tool for identifying proteins in specific tissues under certain conditions. In plants, the proteomic approach has been employed to study alterations in cellular protein expression in response to various biotic and abiotic stresses (Canovas *et al.*, 2004; Gallardo *et al.*, 2003; Shen *et al.*, 2003). More recently, proteomic analysis has been applied to identify proteins associated with plasmodesmata in *Chara corallina* (Faulkner *et al.*, 2005). Previous investigations suggested that pollen-tube development can respond to inhibitor treatments with changes in the expression of a large number of genes that are subjected to either up- or downregulation (Fernando *et al.*, 2001; Hao *et al.*, 2005). Proteomics provides a deeper exploration of pollen-tube development through their protein composition and quantity (Dai *et al.*, 2006; Fernando, 2005; Wilkins *et al.*, 1996). In the present study, 2-DE and mass spectrometry (MS) were used to identify and analyse differentially expressed proteins in the pollen tubes following inhibition of actin polymerization with LATB. The objective of this study was to broaden our understanding of the multiple functions of the actin cytoskeleton at the protein level during pollen germination and tube development in *Picea meyeri* Rehd. et Wils., and to gain insights into protein-expression patterns resulting from actin disruption. The long-term objective of our research is to provide reference maps of pollen proteins with a focus on the effects of environmental and developmental changes during pollen germination and tube growth.

Results

LATB inhibits pollen-tube development and disrupts the actin cytoskeleton

Inhibition of actin polymerization by biochemical agents has a profound effect on pollen-tube growth, leading to disorganization of actin and consequent growth arrest. Usually, *P. meyeri* pollen begins to germinate 14 h after incubation in a culture medium. At concentrations lower than 20 nM, LATB did not delay germination but produced a pronounced effect on maximum tube length (Figure 1). The half-maximal inhibition of pollen-tube growth occurred at a concentration of 20 nM LATB, while pollen germination was completely blocked at concentrations >150 nM.

In a normal germination medium, pollen tubes appeared healthy and had a typical shape. As shown in Figure 2(a), control pollen tubes were long with a constant diameter and clear zone at the tip. In the presence of 20 nM LATB, pollen tubes were substantially shorter and the apex was swollen compared with untreated pollen tubes (Figure 2b). At 50 nM LATB, pollen germination was markedly delayed; after 28 h incubation at this concentration small protrusions appeared, but further tube elongation was inhibited (Figure 2c). At

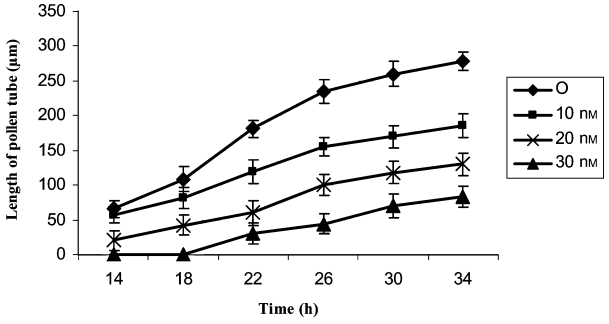

Figure 1. Effects of different concentrations of LATB on the average growth rate of pollen tubes in *Picea meyeri*.

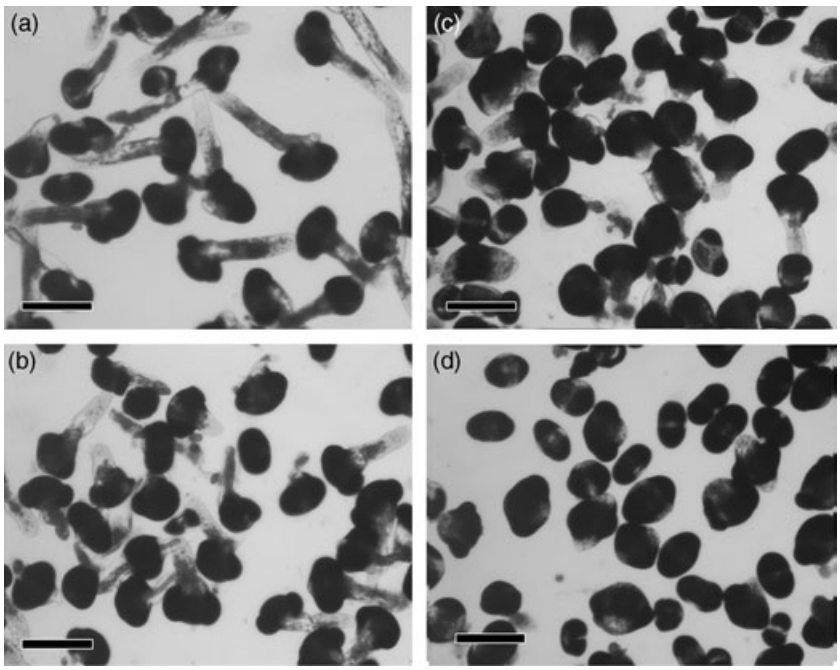

Figure 2. Micrographs of *Picea meyeri* pollen in the presence of LATB.
(a) Control pollen tubes elongated in standard medium for 28 h showing normal shape and lengths.
(b) Pollen tubes were substantially shorter and swollen in the presence of 20 nM LATB for 28 h.
(c) Pollen tubes showing small protrusions in the presence of 50 nM LATB for 28 h.
(d) Pollen cultured in the presence of 100 nM LATB for 28 h. Note that germination was almost entirely blocked. Bar = 100 μm.

100 nM LATB, pollen germination and tube growth was half-maximally inhibited (Figure 2d).

Under the confocal microscope, the actin filaments of untreated pollen tubes incubated in a culture medium for 28 h appeared in an axial array (Figure 3a). A 'collar' of actin, or a dense array of fine filaments, was frequently observed about 20 μm behind the apex of the pollen tube, and a few thick filaments extended beyond the collar into the apex (Figure 3a,b). In the presence of 20 nM LATB, the organization was obviously disturbed, resulting in a meshwork of short actin filaments; furthermore, the collar of actin filaments behind the tip was completely eliminated (Figure 3c,d). In a LATB concentration of 50 nM, only a few, very short actin filaments developed (Figure 3e). When pollen was incubated with 150 nM LATB, these short actin filaments disappeared, probably due to the disruption of F-actin. Only diffuse fluorescence aggregates of phalloidin-stained material were found (Figure 3f) instead of the well defined fluorescent filaments typical in control pollen tubes.

Effects of LATB on the ultrastrucure of pollen tubes

A clear zone, filled mainly with secretory vesicles, was identified at the very tip of pollen tubes growing in control medium. Behind this tip were larger organelles such as Golgi stacks, endoplasmic reticulum (ER) and mitochondria, as well as many small, round-shaped vacuoles (Figure 4a). The Golgi stacks had six to eight tightly packed cisternae and were surrounded by numerous secretory and coated vesicles (Figure 4c). A majority of the mitochondria had abundant cristae and an electron-dense matrix (Figure 4g). The starch granules of amyloplasts were discoid, with an average cross-sectional area of 7.71 μm^2 ($n = 110$) (Figure 4k). The LATB treatment disrupted the polarized organization of the cytoplasm, leading to the shift of larger organelles such as mitochondria and lipid bodies at the tip (Figure 4b). The disruption of the actin cytoskeleton caused a dramatic effect on the ultrastructure of the Golgi apparatus, mitochondria and starch grains. The severity of these effects depended on the concentration of LATB. After treatment with 20 nM LATB for 6 h, Golgi cisternae were slightly swollen, loose and fragmented (Figure 4d), while only slight changes were observed in mitochondrial cristae (Figure 4h). Treatment for 28 h resulted in a lower number of Golgi cisternae, which were also disintegrated and fragmented, and a dramatic drop in the number of secretory vesicles (Figure 4e). Simultaneously, the mitochondrial membranes showed damage, including a drastically reduced number of cristae (Figure 4i). At a LATB concentration of 50 nM for 28 h, both Golgi and mitochondrial membranes were completely disintegrated, mitochondrial cristae disappeared (Figure 4f,j), and starch grains were reduced in size (Figure 4l) with an average cross-sectional area of 2.85 μm^2 ($n = 169$). These data clearly indicate that actin, in addition to aiding Golgi motility, is also important for maintaining the integrity of the Golgi apparatus.

Proteomic profiles of germinating pollen in P. meyeri *following inhibition of actin polymerization*

Proteins were extracted from pollen 6, 12, 18 and 28 h after treatment with two concentrations of LATB (20 and 50 nM) to

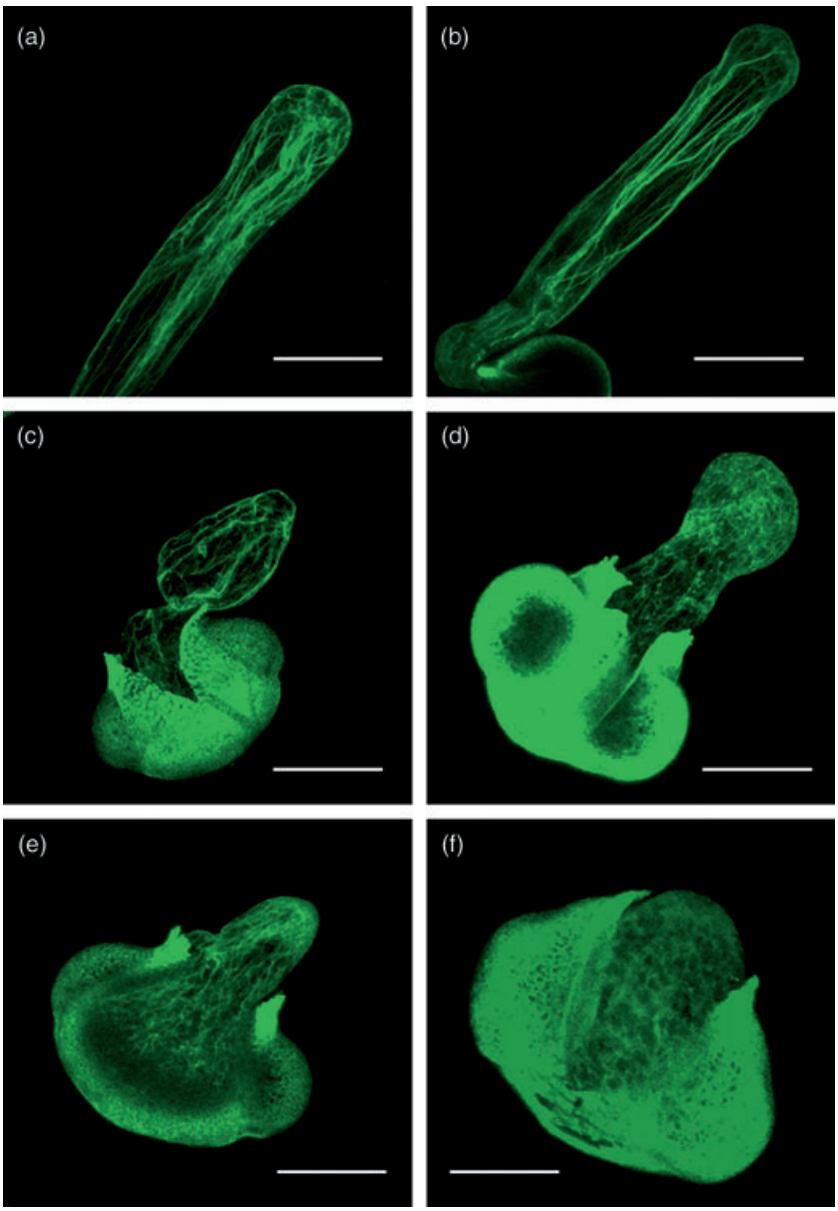

Figure 3. Effect of LATB on the inhibition of F-actin polymerization in *Picea meyeri* germinating pollen and pollen tubes. Actin labelling with phalloidin-TRITC is shown in pseudo green colour.
(a, b) Untreated pollen cultured in standard medium for 18 and 28 h showing long pollen tube and normal organization of actin filaments and bundles.
(c) Pollen treated with 20 nM LATB for 18 h. Actin filament organization has been disturbed and did not show thick longitudinal bundles.
(d) Pollen treated with 20 nM LATB for 28 h. Inhibition of growth is accompanied by pollen-tube swelling and appearance of diffuse actin fluorescence at the tip, as well as by reorganization of the actin cytoskeleton in the form of short actin microfilaments.
(e) Pollen treated with 50 nM LATB for 28 h. Pollen-tube elongation was considerably inhibited and the actin cytoskeleton appeared in the form of very short microfilaments and aggregates of phalloidin-stained material in the cytoplasm.
(f) Pollen treated with 150 nM LATB for 28 h. Pollen germination was inhibited almost entirely; the intensity of the phalloidin-staining was generally less than in control tubes and tubes treated with lower concentrations of LATB. Bar = 30 μm.

investigate protein alterations as primary and secondary responses to actin disruption. Appropriate controls were treated with 0.5% dimethyl sulfoxide (DMSO), representing the concentration used for 50 nM LATB dilution. Both control and treatment groups were observed at each time point to distinguish between responses to actin disruption and normal developmental changes in protein accumulation. The proteins were separated by 2D gel electrophoresis and visualized with Coomassie Brilliant Blue (CBB) staining, and were subjected to visual assessment to detect differences in the expression levels between pairs of LATB-treated versus control samples.

Reproductive protein expression profiles and nearly 600 spots were resolved on 2D gels over a pH range of 3–10. Most spots were around p*I* 4–8, with molecular weights in the range 14–97 kDa. While the global pattern of pollen tube proteins was largely unaltered (approximately 98% of the total protein spots remained unchanged), 84 protein spots responded to LATB by either up- or downregulation. Subsequently, all these differentially displayed proteins were excised from the gels and subjected to in-gel digestion and mass spectrometry. Automated MASCOT software was used to search protein databases. An example of annotated pollen 2D patterns is shown in Figure 5, and all proteins identified are listed in Table 1. Selected parts of the gels are highlighted in Figure 6 to indicate the time-dependent changes of the actin cytoskeleton after disruption of the responsive protein spots that were obtained from LATB treated and untreated

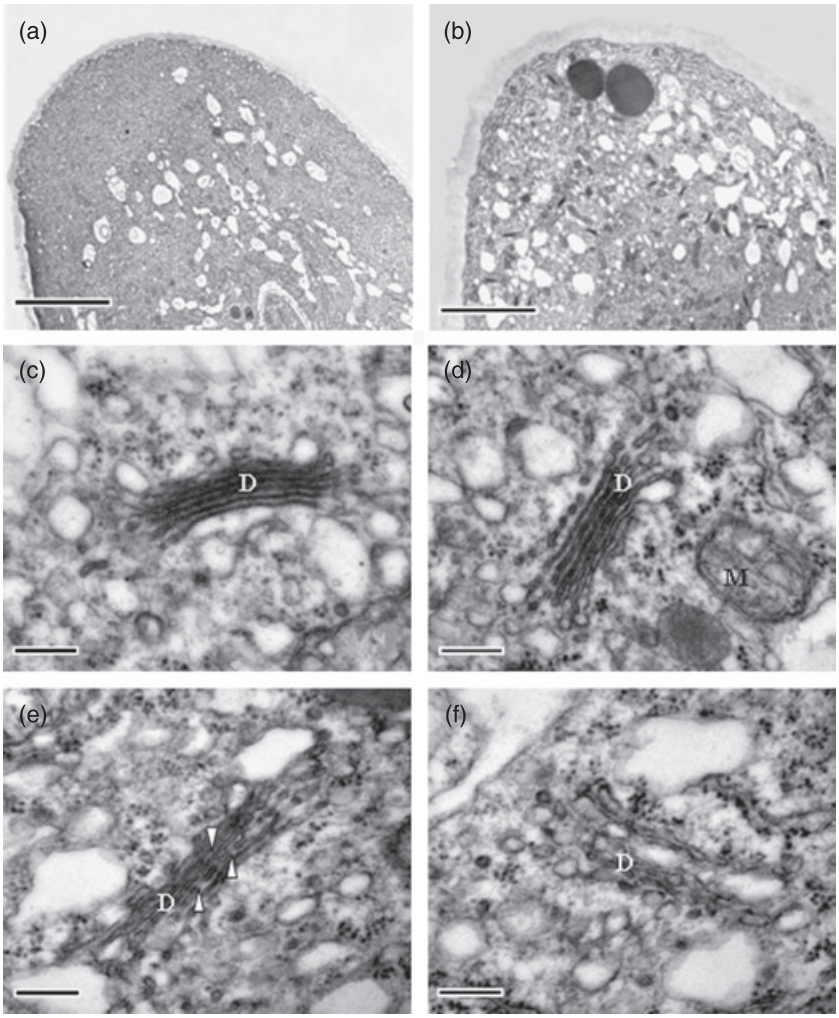

Figure 4. Electron micrographs of normal and LATB-treated pollen tubes.
(a) Apical region of a normal pollen tube cultured for 28 h, showing the apical clear zone.
(b) Tip region of a LATB-treated pollen tube after 20 nM LATB treatment for 28 h. Few secretory vesicles could be observed, while large organelles such as mitochondria, starch grains and lipid bodies appeared.
(c) Typical Golgi stack in a normal pollen tube. It has tightly packed cisternae and numerous secretory vesicles and coated vesicles around it.
(d) Golgi stack in a pollen tube after 20 nM LATB treatment for 6 h. The Golgi cisternae appeared slightly swollen and loosened, while the outermost ones became fragmented.
(e) Golgi stack in a pollen tube after 20 nM LATB treatment for 28 h, showing fragmented cisternae (arrowhead) and reduced number of secretory vesicles.
(f) Golgi stack in a pollen tube after 50 nM LATB treatment for 28 h. Note that Golgi was seriously disaggregated and several cisternae were lost.
(g) Mitochondria in a normal pollen tube. Note that mitochondria had abundant cristae and dense matrix.
(h) Mitochondria in a pollen tube after 20 nM LATB treatment for 6 h, with little change in structure. Note that most membranes remained intact.
(i) Mitochondria in a pollen tube after 20 nM LATB treatment for 28 h, showing partially damaged membranes and reduced number of cristae.
(j) Mitochondria in a pollen tube after 50 nM LATB treatment for 28 h, showing disintegrated membranes and no distinct cristae.
(k) Starch granules in a normal pollen tube cultured for 28 h. Note that starch granules are discoid with a clear and smooth outline.
(l) Starch granules in a pollen tube after 50 nM LATB treatment for 28 h, showing much decreased size with irregular outline.
Bars: (a, b) 5 μm; (c–j) 0.2 μm; (k, l) 1 μm. M, mitochondrion; G, Golgi stack; S, starch granule.

P. meyeri pollen tubes. Because of the lack of a genome sequence of conifers and very low abundance of some proteins, only 53 of the 84 spots tested were found to be identical to those already reported in the NCBInr database. Nevertheless, many genes for abundant proteins appeared to be highly conserved in plants. Among the proteins identified, 16 (30%) were previously reported in conifers; 37 (70%) were highly homologous with those of other plants. Multiple spots in the same pattern may represent a single protein, such as spots 20 and 21, due to post-translational modifications or chemical modifications during sample preparation. In general, conifer pollen responded to actin disruption by upregulation of signalling proteins (quick primary response) and those proteins involved in amino acid/protein synthesis, RNA binding and storage proteins (gradual secondary response). In contrast, some proteins

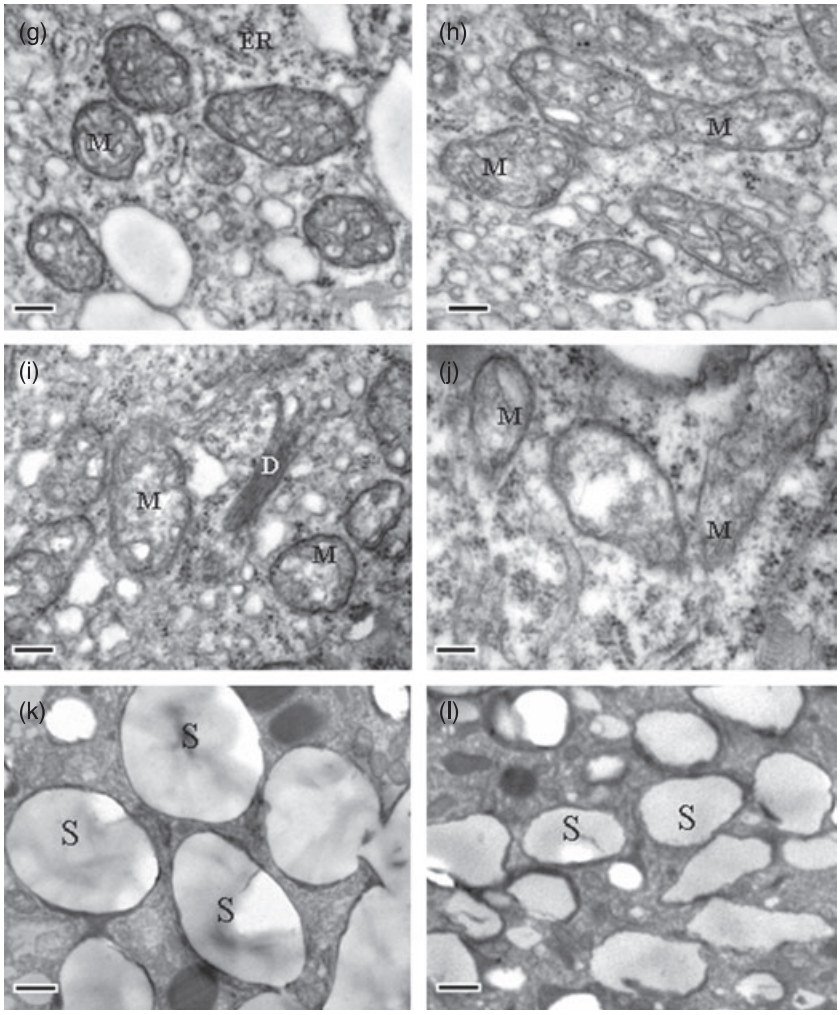

Figure 4. Continued.

involved in signalling, vesicular trafficking and metabolism (quick primary response), along with actin, actin-binding proteins and cell wall proteins involved in cell expansion (gradual secondary response), were downregulated.

Quantitative analysis of protein expression under different time exposures and varying doses of LATB

Proteins extracted at 6, 12, 18 and 28 h treatment under two concentrations of LATB and appropriate controls were compared by differentially displayed proteomic analysis to identify the primary response of pollen tube to actin disruption. The time-course experiments revealed that most of the differentially expressed proteins showed quantitative changes in a time-dependent manner. Although there was little change in protein accumulation profiles between controls and groups treated with 20 nM LATB up to 6 h, the changes became more pronounced in time and maximized at 28 h. A total of 53 protein spots showed dramatic and reproducible changes, among which 26 were differentially displayed at different times after actin disruption. Some of the down- and upregulated proteins showed rapid quantitative change, >50%, between 6 and 12 h after actin disruption. In contrast, five downregulated proteins (spots 41, 47, 50, 51 and 52) showed qualitative changes between the control and treated samples (Figure 7) and almost disappeared with constant LATB treatment. The expression patterns of several protein spots were dramatically different from most other responses. For example, spot 3 first appeared at 12 h, and its expression increased with time to 28 h of treatment. Because it was visible only in the treated samples, this protein was either synthesized after actin disruption or present in the control in undetectably low abundance. The expression of spots 27 and 50 was reduced to the lowest level at 12 h followed by an increase at 18 and 28 h, but was still lower than in the control. The expression of spot 2 increased until 18 h, when it peaked and then decreased with time to 28 h.

Similarly to the time-dependent changes in protein expression, different doses of LATB led to varying changes

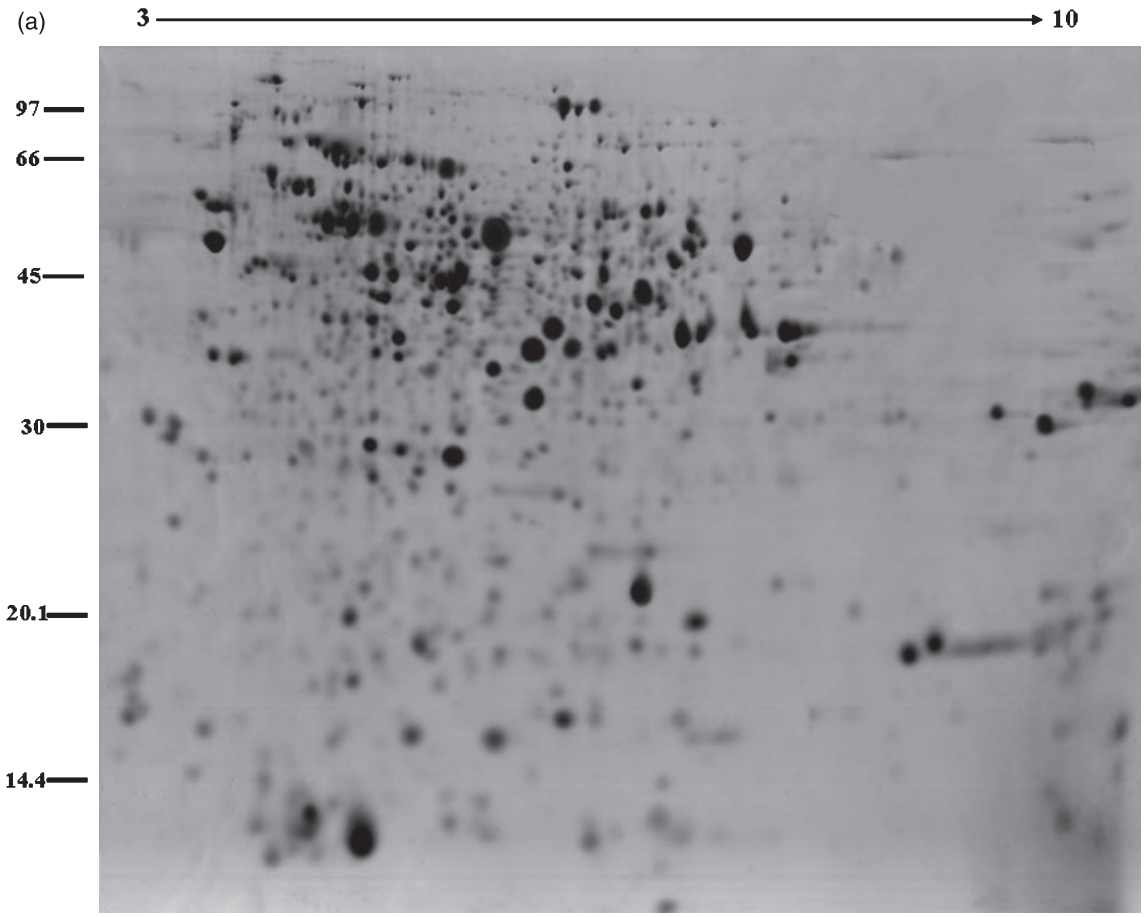

Figure 5. Representative 2-DE gels of pollen proteins.
Pollen was treated with 20 nM LATB for 6 h. Differentially expressed protein spots are indicated by arrows. (a) Pollen proteins without LATB treatment; (b) 25 upregulated protein spots; (c) 28 downregulated protein spots. Some selected regions are enlarged and shown in Figure 6.

in protein expression. The comparative analysis of CBB-stained gels showed that the differential synthesis of proteins responsive to LATB was dose-dependent, with the most marked changes at a concentration of 50 nM LATB treatment. Of the protein spots identified, 53 proteins responded to varying LATB concentrations by up- or down-regulation. Importantly, these changes were fully reproducible and their intensity was clearly dependent on the concentration of LATB. The 26 differentially expressed proteins from the time-treated samples (Figure 7) displayed the same tendency here, while others were not up- or downregulated until 50 nM LATB at 28 h. Interestingly, some proteins (spots 3 and 51) were found to be strongly induced or reduced under mild concentrations (20 nM LATB), then maintained at a constant level even if exposed to a higher and longer treatment (28 h and 50 nM LATB).

Functional significance of differentially expressed proteins

At a functional level, the proteins identified in this study are involved in a wide variety of cellular processes, emphasizing the range of changes associated with the dynamics of an actin cytoskeleton. Moreover, those proteins are also found in different subcellular locations. For example, myosin and profilin bind directly to actin; somatic embryogenesis receptor kinase 1 is associated with endosomes and plasma membrane (Kwaaitaal *et al.*, 2005); luminal binding proteins are localized within the lumen of ER; ATP synthase beta subunits are associated with mitochondrial membrane; reversibly glycosylated polypeptide is present in the Golgi apparatus; carbohydrate metabolism enzymes are cytosolic. The 53 proteins identified were classified into nine major categories according to their presumed biological function (Figure 8).

Functional categorization, either by gene sequence or conserved domain homology with other known proteins, is often based on automated annotation. Many proteins could be identified based on homology (Figure 8). However, some of those listed do not appear to have any prior implication in pollen germination and tube elongation, such as the RNA-binding proteins (spots 18, 19, 20 and 21). Sometimes the significance of the differential display of few proteins on

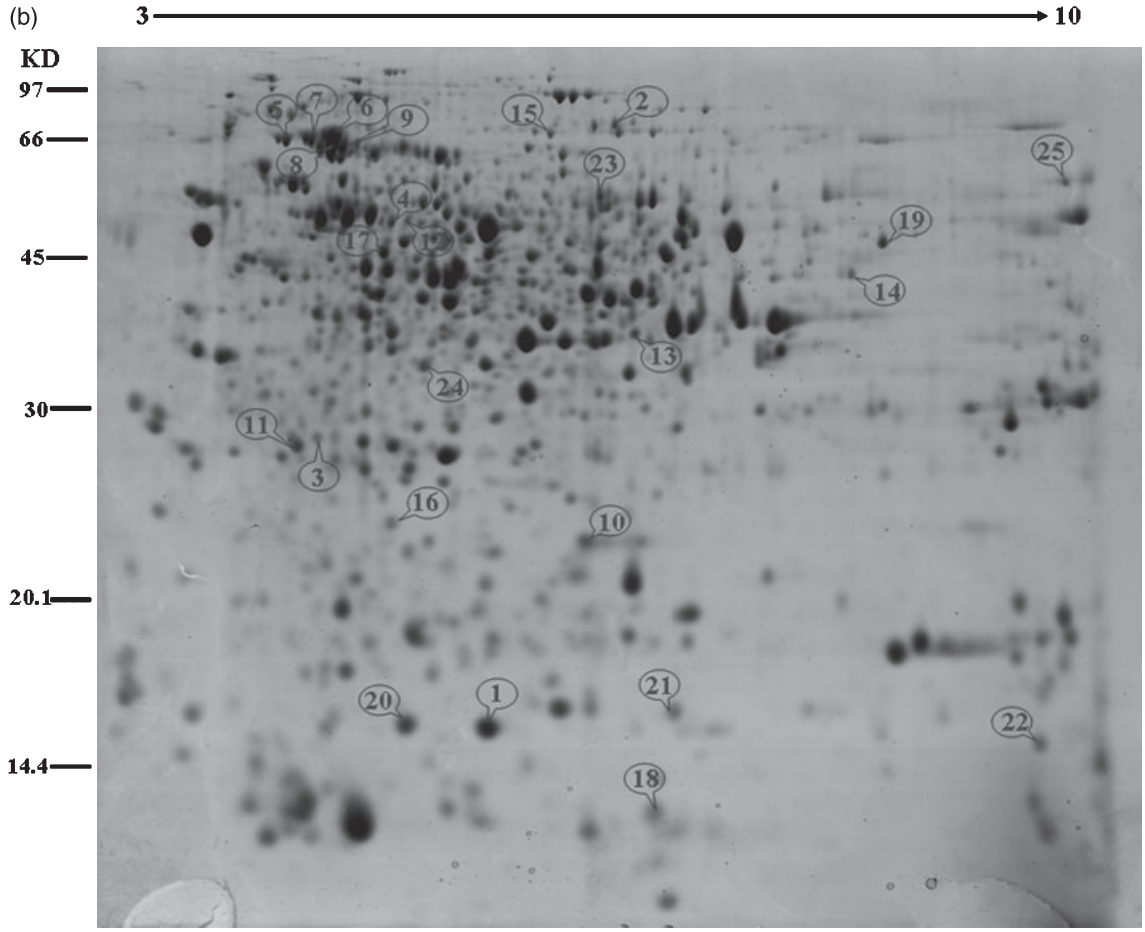

Figure 5. Continued.

LATB is not always clear. For example, phenylcoumaran benzylic ether reductase homologue TH7 (spots 43 and 44) has been shown to represent a new family of pollen-related food allergens that occur not only in pollen, but also in a few allergenic fruits and vegetables (Karamloo *et al.*, 2001). In addition, two proteins identified in this study, spots 24 and 25, have no proven biological function.

Discussion

Pollen-tube elongation has been shown to be affected by a number of factors, including temperature, medium osmolarity and ionic gradients (Franklin-Tong, 1999; Lancelle and Hepler, 1992). Previous investigations revealed that both pollen germination and pollen-tube growth require an intact actin cytoskeleton (Franke *et al.*, 1972; Gibbon *et al.*, 1999). In the present study, we found that LATB disrupted the actin cytoskeleton and markedly suppressed pollen germination and tube elongation in *P. meyeri*. We also found that pollen germination was less sensitive (approximately 10-fold) than tube growth to the disruption of the actin cytoskeleton, similarly to previous studies on maize pollen tubes (Gibbon *et al.*, 1999). More importantly, we found that pollen germination and tube growth in gymnosperms have a different sensitivity to LATB than angiosperms such as maize, which require about three times the level of LATB for a similar result (Gibbon *et al.*, 1999). Thus pollen germination in *Picea* was half-maximally inhibited by 100 nM LATB (compared with 50 nM in maize), while pollen-tube growth was half-maximally inhibited by approximately 20 nM LATB (5 nM in maize). This may have been attributable to differences in pollen/pollen tube cytoskeletal and cytoplasmic organization, modes of cytoplasmic streaming, cell wall permeability, and different germination and pollen-tube growth rates.

Evidence from other plant and eukaryotic cells increasingly suggests that the actin cytoskeleton acts not only as a structural element, but also as the target of signalling pathways (Franklin-Tong, 1999; Šamaj *et al.*, 2002; Staiger, 2000; Volkmann and Baluška, 1999). Transcriptomic analysis revealed that the largest single class of genes expressed in pollen tubes encodes signal transducers, reflecting the necessity to decode the complex and diverse pathways associated with tip growth (Feijó *et al.*, 2004). Proteomic studies complement genomic studies showing protein

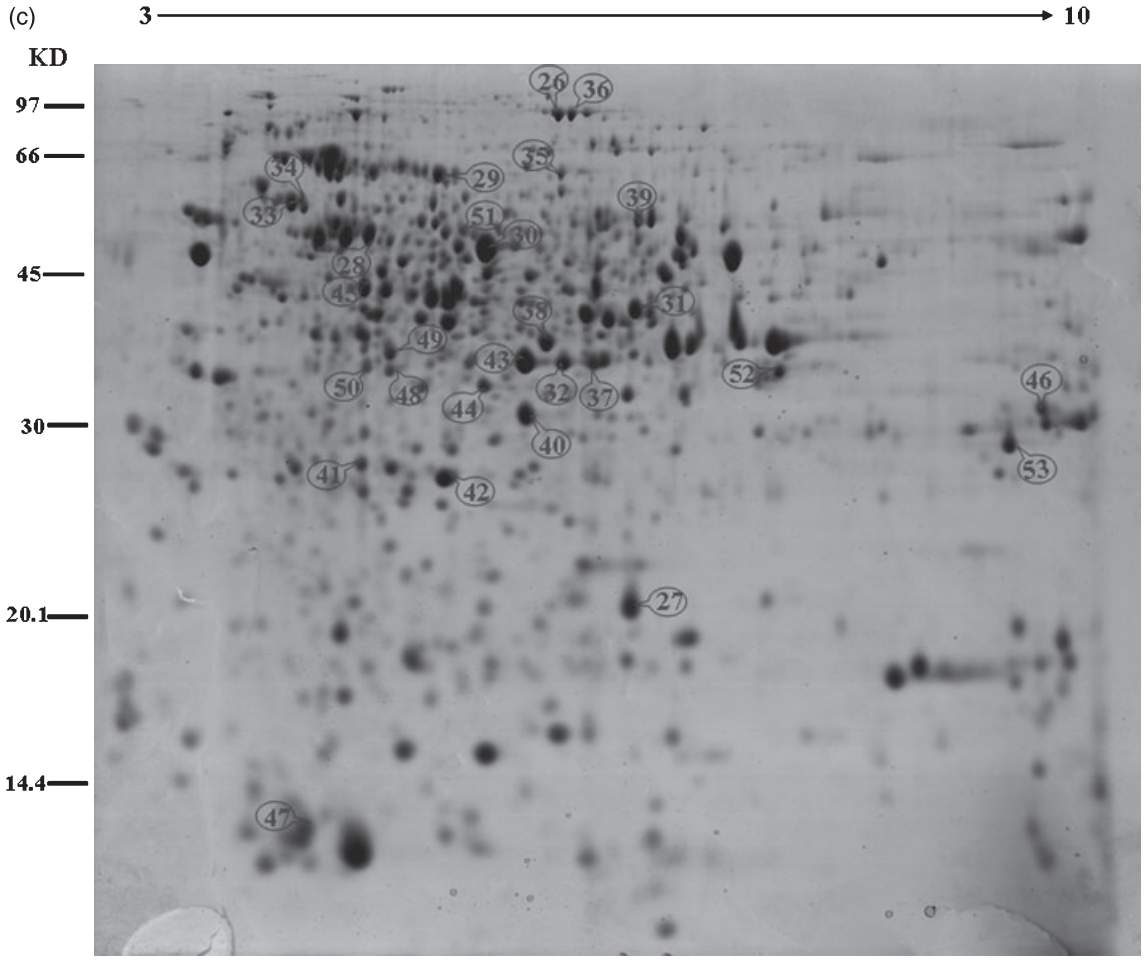

Figure 5. Continued.

changes in response to actin disruption. As LATB has a high affinity for monomeric G-actin, the treatment of pollen with LATB will have a dramatic effect on the function of actin (Vidali *et al.*, 2001). This report presents the systematic analysis of pollen proteome following disruption of F-actin due to LATB, allowing us to classify the individual responsive proteins functionally. To explain the characteristics of these proteins, several categories are discussed separately in relation to their possible roles in the organization and signalling to the actin cytoskeleton.

Signalling proteins

Reversible protein phosphorylation is the most common mechanism for signal transduction. Protein kinases frequently exert their biological effects by creating docking sites for interaction domains, with selectively recognized phosphorylated motifs in their binding partners (Pawson and Nash, 2003). In the present study, inhibition of actin polymerization by LATB led to the differential display of three protein kinases [nucleoside diphosphate kinase B, putative somatic embryogenesis receptor kinase 1, and a mitogen-activated protein kinase (MAPK)-like protein], one putative tyrosine phosphatase, and a putative 14-3-3 protein and calreticulin (a major Ca^{2+}-binding protein).

Putative somatic embryogenesis receptor kinase 1 (SERK1) is involved in brassinosteroid signalling and displays serine/threonine kinase activity (Shah *et al.*, 2001). SERK1 accumulates in endocytic brefeldin A compartments (Kwaaitaal *et al.*, 2005), and this recycling pathway is dependent on F-actin (Murphy *et al.*, 2005; Šamaj *et al.*, 2004). Moreover, endosomes in plant cells use actin polymerization for motility (Voigt *et al.*, 2005). Because SERK1 is already present in pollen grains, it can be assumed that the actin cytoskeleton in germinating pollen is involved in the SERK signalling pathway, and disruption of F-actin results in its downregulation.

In higher plants, MAPK cascades minimally consist of a MAP3K–MAP2K–MAPK module linked in various ways to upstream receptors and downstream targets, including the actin cytoskeleton (Šamaj *et al.*, 2004). Cross-talk between activated MAPK and the actin cytoskeleton is essential for tip

Table 1 Mass spectrometry matching of LATB-upregulated or downregulated proteins in *Picea meyeri* pollen tubes

Spot ID	Protein	Obs. p*I*/M_r	Theor. p*I*/M_r	Accession number	SC (%)	Organism	MASCOT score	Location	Possible function	Identification method
Upregulated proteins										
Signalling proteins										
1	Nucleoside diphosphate kinase (NDP kinase B)	5.9/15	6.43/16.19	P47920	36	*Flaveria bidentis*	272	Cytoplasm	Signal transduction	PMF, MS/MS
2	Putative tyrosine phosphatase	6.6/78	5.11/71	AAN41331	10	*Arabidopsis thaliana*	67	Cytoplasm	Signal transduction	PMF MS/MS
3	Putative 14-3-3 protein	5/29	4.81/29.16	XP-469508	36	*Oryza sativa*	525	Cytoplasm	Signal transduction	MS/MS
4	Calreticulin	5.3/47	4.6/49.6	AAG01147	4	*Pinus taeda*	102	ER	Signal transduction	MS/MS
Proteins involved in protein synthesis, processing and transport										
5	Luminal binding protein	4.7/81	5.15/74.9	CCA89834	10	*Pseudotsuga Menziesii*	651	ER	Protein folding and degradation	PMF, MS/MS
6	Luminal binding protein	4.9/70	5.15/74.7	Q40924	10	*Pseudotsuga menziesii*	67	ER	Protein folding and degradation	PMF
7	Heat-shock protein 70	4.8/70	5.08/73.5	CAB72128	12	*Cucumis sativus*	70	ER	Protein folding and degradation	PMF
8	dnaK-type molecular chaperone HSP71.2	4.9/68	5.17/71.1	CAA31663	10	*Petunia* × *hybrida*	69	ER	Protein folding and degradation	PMF
9	dnaK-type molecular chaperone HSP71.2	5.0/68	5.17/71.1	CAA31663	10	*Petunia* × *hybrida*	69	ER	Protein folding and degradation	PMF
10	Mitochondria-localized low molecular-weight heat-shock protein 23.5	7.2/22	8.76/23.54	AAB01557	15	*Picea glauca*	133	M	Protein folding and degradation	PMF, MS/MS
11	Protein disulfide-isomerase	4.3/56	4.45/55.56	S62626	10	*castor bean*	226	Cytoplasm	Protein folding and degradation	MS/MS
12	Putative mitochondrial processing peptidase	5.0/50	5.95/54.2	BAD86941	20	*Oryza sativa*	228	M	Protein folding and degradation	MS/MS
13	Protein synthesis elongation factor Tu	6.7/32	4.9/25.7	AAA87701	40	*Koliella longiseta*	70	Cytoplasm	Protein biosynthesis	PMF
Amino acid synthesis proteins										
14	asp aminotransferase	8.2/43	8.21/51.1	1908424A	7	*Medicago sativa*	120	Cytoplasm	Amino acid biosynthesis	MS/MS
15	Cobalamine-independent methionine synthase	6.0/81	6.17/86.72	CAA89019	10	*Solenostemon scutellarioides*	250	Cytoplasm	Amino acid biosynthesis	MS/MS
16	Methionine synthase	5.3/24	5.69/24.4	AAF26735	11	*Coffea arabica*	162	Cytoplasm	Amino acid biosynthesis	MS/MS
17	S-adenosylmethionine synthetase	5.3/46	5.55/43.5	AAG17036	16	*Pinus contorta*	76	Cytoplasm	Amino acid biosynthesis	PMF, MS/MS

Table 1 Continued

Spot ID	Protein	Obs. p*I*/M_r	Theor. p*I*/M_r	Accession number	SC (%)	Organism	MASCOT score	Location	Possible function	Identification method
RNA-binding proteins										
18	RNA-binding protein	5.8/14	6.81/13	E86458	40	*Arabidopsis thaliana*	80	Nuclear	Transcription	PMF
19	Putative RNA-binding like protein	8.8/47	9.03/57.78	CAA44874	15	*Oryza sativa*	68	Nuclear	Transcription	MS/MS
20	Glycine-rich RNA-binding protein	5.4/16	7.57/15.4	AAD28176	47	*Picea glauca*	492	Nuclear	Transcription	PMF, MS/MS
21	Glycine-rich RNA-binding protein	7.2/15	7.9/15.5	AAD28176	45	*Picea glauca*	114	Nuclear	Transcription	PMF, MS/MS
Storage proteins										
22	Late embryogenesis abundant protein	8.2/15	8.92/15.75	2211386D	29	*Pseudotsuga menziesii*	317	Cytoplasm	Storage	MS/MS
23	Legumin-like storage protein	6.9/55	7.09/57.37	CAA44874	21	*Picea glauca*	163	Cytoplasm	Storage	MS/MS
Unclassified proteins										
24	Unnamed protein product	5.5/34	5.2/34.2	NP_914531	19	*Oryza sativa*	65	peroxisome	Unknown	PMF
25	Hypothetical protein	9.0/91	8.9/87.5	NP_922554	10	*Oryza sativa*	66	Cytoplasm	Unknown	PMF
Downregulated proteins										
Signalling proteins										
26	Putative somatic embryogenesis receptor kinase 1	6.4/80	5.9/69.1	XP_480325	15	*Oryza sativa*	67	plasma membrane	Signal transduction	PMF
27	MAP kinase-like protein	6.9/21	7.08/22.84	AAB57843	8	*Selaginella lepidophylla*	67	Cytoplasm	Signal transduction	MS/MS
Metabolic enzymes										
28	Mitochondrial ATP synthase beta subunit	5.2/55	5.95/60.2	CAA41401	17	*Heyea brasiliensis*	70	M	Energy pathway	PMF
29	Phosphoglycerate mutase, 2, 3-bisphosphoglycerate-independent	5.4/60	5.29/60.75	A42807	5	*Maize*	169	Cytoplasm	Glycolysis	PMF, MS/MS
30	Pollen 2-phosphoglycerate dehydrogenase 2 precursor	5.9/51	5.70/48.42	AAQ17040	27	*Cynodon dactylon*	629	Cytoplasm	Glycolysis	PMF, MS/MS
31	NAD-dependent glyceraldehyde-3-phosphate dehydrogenase	7.0/39	8.69/39.29	CAA04942	12	*Pinus sylvestris*	133	Cytoplasm	Glycolysis	PMF, MS/MS
32	Fructose-1,6-diphosphate aldolase	6.0/34	9.3/34.48	AAM81204	11	*Metasequoia glyptostroboides*	114	Cytoplasm	Glycolysis	MS/MS
33	Starch synthase	4.7/64	7.47/67.93	AAA86423	5	*Ipomoea batatas*	157	Cytoplasm	Glycolysis	PMF, MS/MS
34	Granule-bound glycogen (starch) synthase	4.7/64	7.56/67	AAC70779	3	*Astragalus membranaceus*	74	Cytoplasm	Glycolysis	MS/MS
35	Pyruvate decarboxylase	6.0/65	5.99/65.4	AAP96920	10	*Dianthus caryophyllus*	95	Cytoplasm	Citrate cycle	MS/MS
36	Aconitate hydratase	6.2/96	5.74/98.57	T10101	3	*Cucurbit*	91	Cytoplasm	Citrate cycle	PMF, MS/MS

Table 1 Continued

Spot ID	Protein	Obs. p*I*/M_r	Theor. p*I*/M_r	Accession number	SC (%)	Organism	MASCOT score	Location	Possible function	Identification method
37	Malate dehydrogenase	7.2/37	8.11/37.49	AAC37464	3	*Glycine max*	82	Cytoplasm	Citrate cycle	PMF, MS/MS
38	Malate dehydrogenase	6.3/36	6.18/35.50	AAR32785	11	*Pinus pinaster*	194	Cytoplasm	Citrate cycle	PMF, MS/MS
39	Mitochondrial aldehyde dehydrogenase RF2B	6.5/52	6.29/58.56	AAL99614	6	*Zea mays*	113	M	Metabolism	PMF, MS/MS
40	Putative thiamine biosynthesis protein	6.2/32	5.44/37.16	XP_478512	8	*Oryza sativa*	124	Cytoplasm	Metabolism	PMF, MS/MS
41	Triosephosphate isomerase	4.8/27	5.54/27.1	CAA58230	15	*Petunia* × *hybrida*	147	Cytoplasm	Metabolism	MS/MS
42	Ascorbate peroxidase	5.7/28	5.4/27.25	AAR32786	15	*Pinus pinaster*	214	Cytoplasm	Metabolism	PMF, MS/MS
43	Phenylcoumaran benzylic ether reductase homologue TH7	6.2/34	6.20/33.89	AAF64182	20	*Tsuga heterophylla*	97	Cytoplasm	Metabolism	PMF, MS/MS
44	Phenylcoumaran benzylic ether reductase	6.0/33	7.46/35.55	AAC32591	14	*Pinus taeda*	207	Cytoplasm	Metabolism	MS/MS
Actin cytoskeleton proteins										
45	Actin	5.2/45	5.3/41.7	T51180	25	*Picea rubens*	389	Cytoskel	Cytoskeleton Dynamics	PMF, MS/MS
46	Myosin-like protein	9.5/36	6.74/39.11	XP_478321	15	*Oryza sativa*	147	Cytoskel	Cytoskeleton Dynamics	MS/MS
47	Profilin	4.9/14	4.91/14.23	AAP52957.1	32	*Ricinus communis*	144	Cytoplasm	Cytoskeleton Dynamics	MS/MS
Cell wall expansion proteins										
48	Type IIIa membrane protein cp-wap13	5.4/39	6.24/40.08	AAB61672	26	*Vigna unguiculata*	514	Golgi	Cell wall remodelling	PMF, MS/MS
49	Reversibly glycosylated polypeptide	5.2/39	5.82/41.98	CAA77237	27	*Triticum aestivum*	461	Golgi	Cell wall remodelling	PMF, MS/MS
50	Golgi-associated protein se-wap41	5.2/38	5.75/41.2	AAB49896	6	*Zea mays*	76	Golgi	Cell wall remodelling	MS/MS
51	UDP-glucose dehydrogenase	6.0/49	5.99/53.5	AAR84297	17	*Cinnamomum osmophloeum*	364	Cytoplasm	Cell wall remodelling	MS/MS
52	Beta-expansin OsEXPB13	8.0/33	8.01/28.7	AAL24476	17	*Oryza sativa*	355	Cytoplasm	Cell wall remodelling	MS/MS
53	Putative proline-rich protein	9.0/28	8.82/23.95	AAP52133	6	*Oryza sativa*	66	Cytoplasm	Cell wall remodelling	MS/MS

Spot ID refers to the number of spots as shown in Figure 5.
Obs. p*I*/M_r, observed p*I*/M_r calculated from the 2D-gels with Image Master 2D PLATINUM 5.0 software according to standard marker proteins.
Theor. p*I*/M_r, theoretical p*I*/M_r, given for proteins with matched proteins.
Accession number, proteins identified by MS and extracted from the National Center for Biotechnology Information (NCBI) database (until October 2005).
SC, sequence coverage. Locations of proteins were identified by WOLF PSORT (http://wolfpsort.seq.cbrc.jp).
ER, endoplasmic reticulum; M, mitochondrion; cytoskel, cytoskeleton.
Identification method: PMF, peptide mass fingerprint; MS/MS, electrospray ionization tandem mass spectrometry.

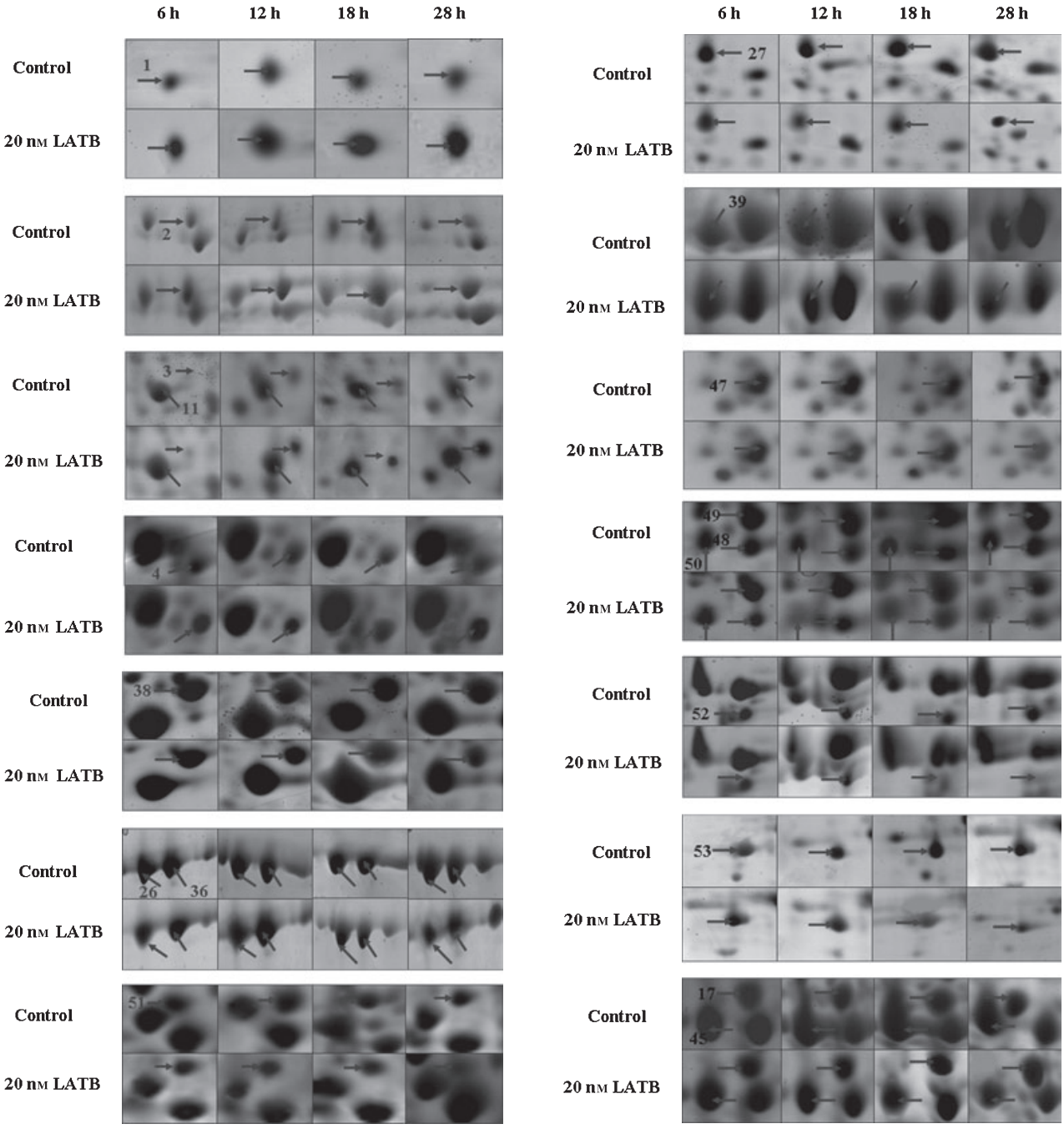

Figure 6. Magnified comparison of some 2-DE gels to show time-dependent changes of the differentially expressed proteins.
Proteins in pollen were extracted from both control and LATB-treated samples after 6, 12, 18 and 28 h treatment, and separated by 2-DE. Protein spot quantification was carried out from at least three gels from each pollen-tube sample. Protein spot numbers as in Table 1.

Figure 6. Continued.

growth of root hairs (Šamaj *et al.*, 2002). Previous studies reported that the MAPK protein is activated shortly after pollen hydration, and plays a role in the germination process of tobacco pollen (Wilson *et al.*, 1997). In this study, we found that actin disruption downregulated MAPK-like protein, suggesting a new link between F-actin and MAPK signalling in germinating *Picea* pollen.

Using the proteomic approach, we found that one protein spot that matched with tyrosine phosphatase was upregulated. Tyrosine phosphatase is known to be expressed exclusively at the later developmental stage in pollen grains (Gupta *et al.*, 2002). MAPK signalling is terminated by the specific action of protein phosphatases, and a MAPK-like

(a)

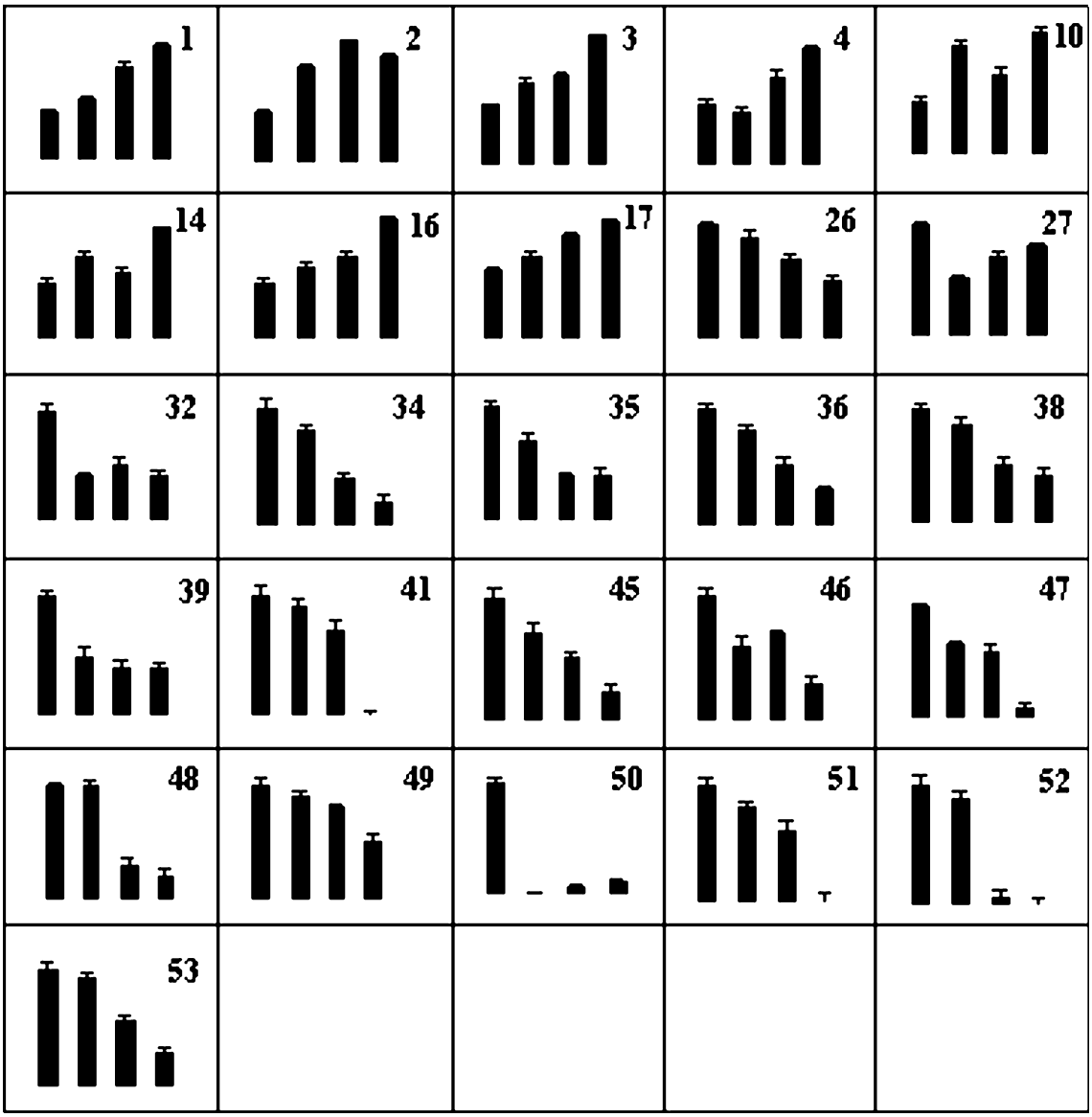

Figure 7. Relative levels of expressed proteins.
Proteins were extracted from pollens, separated by 2D-PAGE and detected by Coomassie Brilliant Blue staining. Following scanning, gel patterns were analysed using the Image Master 2D PLATINUM 5.0 software, and the relative abundance ratio of proteins was determined.
(a) Pollen proteins in the presence of 20 nM LATB for 6 h (column 1); 12 h (column 2); 18 h (column 3); 28 h (4).
(b) Pollen-tube proteins in the presence of 0 nM LATB (column 1); 20 nM LATB (column 2); 50 nM LATB (column 3) cultured for 28 h.

protein was found to be downregulated in a correlative manner upon actin disruption. Thus localization and/or the activity of this phosphatase may be dependent on intact F-actin. Plant actin is known to be phosphorylated on tyrosine residues during development, which controls the bending of plant petioles (Kameyama *et al.*, 2000). A recent study revealed specific actin phosphorylation on tyrosine residue during embryo imbibition and germination in maize (Diaz-Camino *et al.*, 2005). Similarly, tyrosine phosphorylation of actin might occur during pollen germination, and actin disruption by LATB may upregulate tyrosine phosphatases responsible for actin dephosphorylation. Thus, tyrosine phosphatase could affect either signalling (e.g. MAPKs) or actin phosphorylation, leading to the inhibition of pollen germination and tube growth.

One protein spot that was exclusively expressed and upregulated by LATB treatment was the 14-3-3 protein. This protein has phosphoserine/threonine-binding properties and binds a wide variety of cellular proteins involved in cell signalling, scaffolding and metabolism comprising at least 0.6% of the cellular proteome (Jin *et al.*, 2004; Meek *et al.*, 2004). It downregulates the ATP synthase beta subunit

(b)

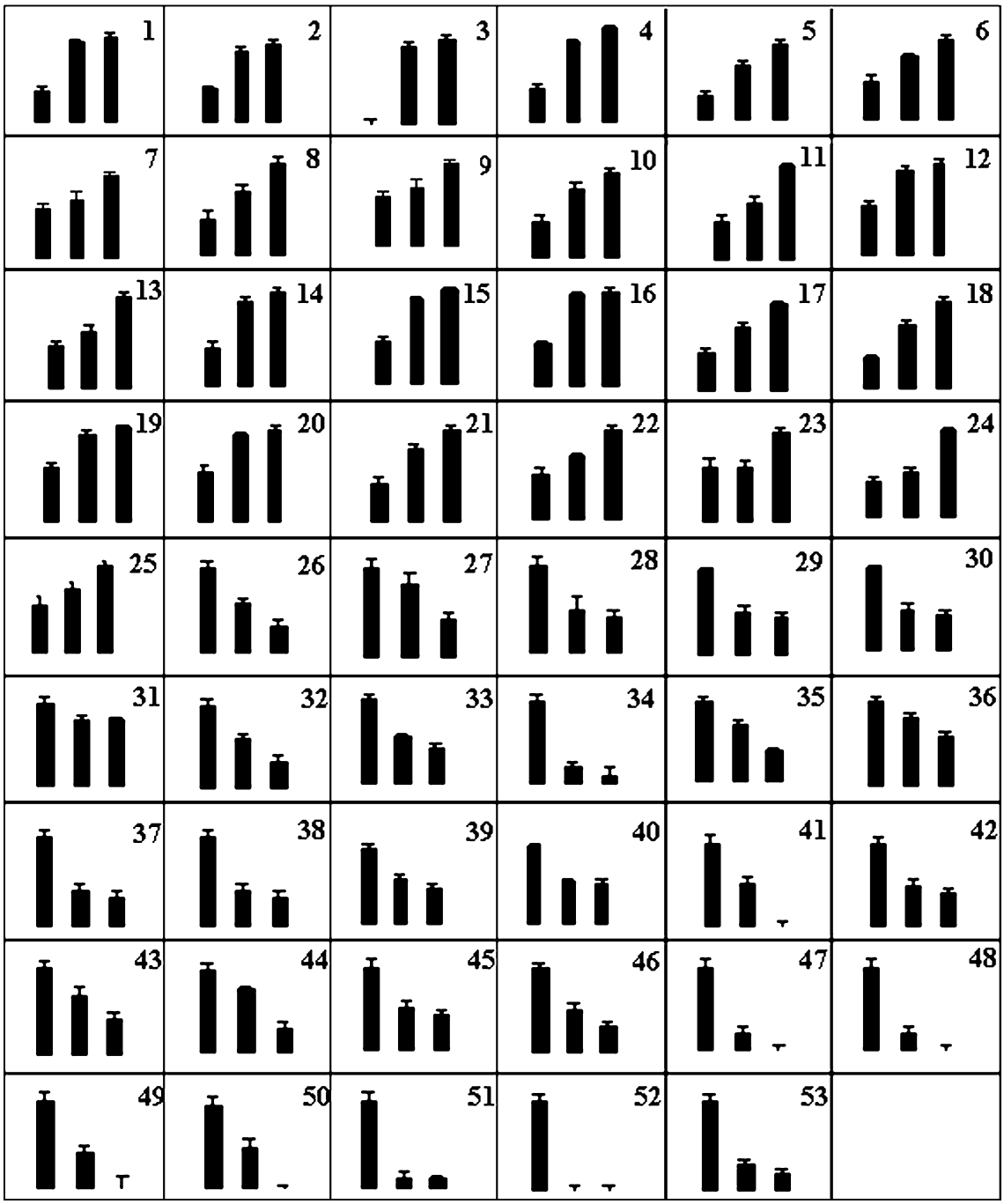

Figure 7. Continued.

(Bunney *et al.*, 2001), which is consistent with the downregulation of mitochondrial ATP synthase (spot 28) accompanied by the disruption of mitochondrial membranes in our experiments (Figure 4g–j). Another possibility is that the upregulated 14-3-3 protein can specifically downregulate the activity of starch synthase (Sehnke *et al.*, 2001), leading to decreased starch deposition, as suggested by our electron microscopic studies (Figure 4k,l) and correlative downregulation of starch synthase (spot 34). Most importantly, Jin *et al.* (2004) recently found that many novel 14-3-3-binding proteins are directly involved in regulating the polymerization of the actin cytoskeleton. Therefore upregulation of the 14-3-3 protein can affect multiple facets of cellular architecture.

Another upregulated protein spot matched to NDP kinase B, a key enzyme in maintaining cellular pools of nucleoside

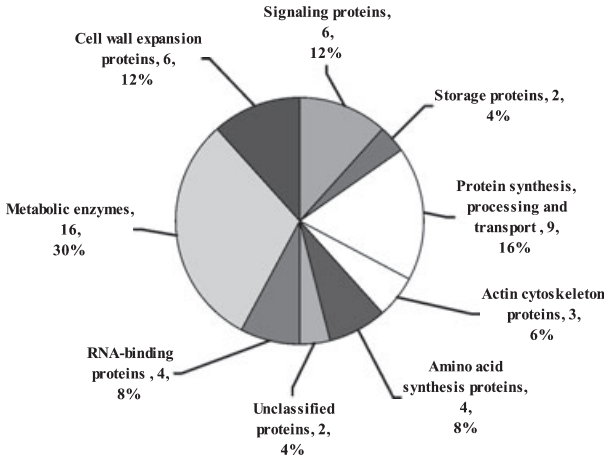

Figure 8. Assignment of identified proteins to functional categories. The total number and percentage of proteins in each functional category were determined.

triphosphates (Parks and Agarwal, 1973). A recent report revealed that NDP kinase B could serve as a both guanine nucleotide-exchange factor and a GTPase-activating protein (Knorpp *et al.*, 2003). The ability of NDP kinase B to supply GTP suggests a role in G-protein-mediated signalling. Because of an increase in NDP kinase B, G-protein expression may be affected in germinating pollen with disrupted F-actin.

In our studies calreticulin, a major Ca^{2+}-sequestering protein that typically resides in the ER lumen, was found to be upregulated. In addition to its acknowledged roles in calcium signalling and storage, calreticulin acts as a chaperone in the quality control of glycoproteins passing through the ER (Camacho and Lechleiter, 1995; Zhang and Salter, 1998). It is well established that the overexpression of calreticulin leads to an increase of Ca^{2+} in the ER and simultaneous depletion in the cytoplasmic signalling pool (Persson *et al.*, 2001). Calreticulin was localized along with F-actin and myosin VIII to the tips of emerging root hairs (Baluška *et al.*, 2000). The cytoplasmic Ca^{2+} gradients at the tip and the actin cytoskeleton are the key factors that control pollen germination and tube growth (Holdaway-Clarke *et al.*, 1997; Pierson *et al.*, 1996). Based on these observations, we can conclude that LATB-induced upregulation of calreticulin may increase Ca^{2+} in the ER, thus modulating downstream processes correlated with cytoplasmic Ca^{2+}-signalling pathways.

Cytoskeletal proteins

Signal transduction cascades converge on the actin cytoskeleton during many fundamental cellular responses. Previous reports have revealed that the actin cytoskeleton and several actin-binding proteins interacting with signalling pathways are involved in the regulation of pollen-tube growth (Staiger, 2000; Staiger *et al.*, 2000). In the tube apex, there is a rapid turnover of actin filaments controlled by actin-binding proteins (Chen *et al.*, 2002; Staiger and Hussey, 2004; Vidali *et al.*, 2001). There is sufficient evidence that pollen profilin is involved in interactions with pollen protein kinases and/or phosphatases to modulate both their activity and the rate of actin polymerization (Clarke *et al.*, 1998). The myosin-like protein is a motor protein that moves along actin filaments by force-generating hydrolysis of ATP (Lee and Liu, 2004). One of the principal functions of motor proteins is to transport the vesicles on actin filaments and retain organelles at specific locations in the cell. The third downregulated spot corresponded to actin, a fundamental component of the cytoskeleton. In angiosperms, LATB has no effect on the synthesis of actin in pollen (Spector *et al.*, 1983). For mature pollen, Callis and Bedinger (1994) demonstrated that actin was highly abundant in a nonfilamentous form ready to be rapidly polymerized during tube germination. This suggests that the synthesis of new protein is necessary only for the subsequent elongation of pollen tubes. In this study, we found that several signalling pathways are altered by the reorganization and disruption of the actin cytoskeleton. Consequently, changes in the dynamic properties of these signalling pathways may use intracellular second messengers for the feedback regulation of actin synthesis. Importantly, the timing of protein synthesis in conifers differs considerably from that reported for angiosperms, where the mature nongerminated pollen grains already contain all the proteins required for germination and early tube elongation. In coniferous species, the initiation of pollen germination and the maintenance of pollen-tube elongation depend on continuous protein synthesis (Fernando *et al.*, 2001; Hao *et al.*, 2005).

Proteins involved in cell wall expansion

The tip growth of pollen tubes is based on processes such as vesicle transport and fusion, expansion of the cell wall and plasma membrane and compensatory endocytosis, which depend on an intact actin cytoskeleton. LATB-inhibited plant cell expansion has been reported in pollen tubes, root apices and root hairs (Baluška *et al.*, 2001; Gibbon *et al.*, 1999; Šamaj *et al.*, 2002; Vidali *et al.*, 2001). However, the impact of actin disruption on proteins involved in secretory pathways and cell wall formation are largely unknown.

We found that actin disruption via LATB resulted in early downregulation of protein spots that matched with Golgi-associated protein se-wap41, type IIIa membrane protein cp-wap13, and reversibly glycosylated polypeptide-1 (RGP1). Sequence comparisons using BLAST searches indicate that type IIIa membrane protein cp-wap13 and Golgi-associated protein se-wap41 show high levels of identity with reversibly glycosylated polypeptide-1 (RGP1). By immunogold labelling, Dhugga *et al.* (1997) showed that RGP1 is specifically

localized to Golgi stacks, where it is likely to be involved in xyloglucan biosynthesis (Sherrier and VandenBosch, 1994). The proteins RGP1 and type IIIa membrane protein cp-wap13 decreased markedly and almost disappeared when the concentration of LATB was increased to 50 nM. Moreover, actin disruption by LATB was accompanied by reorganization, fragmentation and disruption of Golgi membranes, as revealed by our transmission electron microscope (TEM) studies.

Three other spots downregulated on LATB treatment matched with proteins involved in either the biosynthesis of cell wall components or cell wall expansion. These included UDP-glucose dehydrogenase (UGDH), beta-expansin OsE-XPB13, and putative proline-rich protein. UGDH plays a key role in the synthesis of cell wall components. As much as 60% of the total polysaccharide content of the cell wall is derived, either directly or indirectly, from UDP-glucuronate (Hempel *et al.*, 1994). We found that two cell wall proteins, beta-expansin and proline-rich protein, were downregulated. Beta-expansins are known as group I grass allergens and cell wall-loosening factors, helping penetration of the pollen tube through stigma and style via softening the maternal cell walls. Proline-rich proteins are expressed in many plant species in a temporally and spatially regulated manner during development, and their expression correlates well with cell expansion. Taken together, these data suggest that actin disruption interferes with the secretory system by disrupting Golgi integrity and function, and by altering the deposition of cell wall components.

Proteins involved in ATP generation, transport and carbohydrate metabolism

Respiration is critical to metabolism in higher plants. In addition to its link with carbon metabolism, respiration releases energy stored in carbon-based compounds in a controlled manner for cellular use. It also generates many carbon precursors for biosynthesis. Pollen-tube growth requires a high rate of carbohydrate metabolism to meet energetic and biosynthetic demands (Hepler *et al.*, 2001), and growing pollen tubes respire at least 10 times faster than green leaf tissue (Tadege *et al.*, 1999). Among differentially displayed proteins of LATB-treated pollen tubes, we identified two general categories containing enzymes of the central metabolic pathways involved in energy production (Figure 5, marked in red). These enzymes were all downregulated in the LATB-treated pollen tubes.

The first group includes one enzyme that was involved in oxidative phosphorylation. It comprises enzymes from different metabolic pathways that are involved in ATP generation and transport, including one special form of mitochondrial ATP synthase beta subunit, which serves as a catalyst in the terminal step of oxidative respiration, converting generation of the electrochemical gradient into ATP for cellular biosynthesis. It was reported recently that ATP synthase is embedded in the inner mitochondrial membranes, where it uses the proton motive force generated across the membrane by respiration to synthesize ATP from ADP and inorganic phosphate (Carbajo *et al.*, 2004). Our TEM observations confirmed that the LATB-induced disruption of mitochondrial membranes correlates with downregulation of ATP synthase.

The second group includes 10 major enzymes involved in the generation of metabolic energy (Figure 9, marked in red). It contains seven key and rate-limiting enzymes involved in glycolysis, and four citrate-cycle enzymes, which regulate the progress of the citric acid cycles and are necessary for regulating carbon flow in the citrate cycle. In addition, a mitochondrial aldehyde dehydrogenase RF2B (ALDH) was identified, which is part of an indirect metabolic pathway for the synthesis of acetyl-CoA, bypassing the direct route via pyruvate dehydrogenase (Figure 9, marked in green).

This decreased synthesis of enzymes suggests dynamic changes in carbohydrate metabolism coupled with energy production due to the loss of intact F-actin. This view is further supported by the downregulation of a coenzyme synthase (thiamine biosynthesis) and a shuttle protein for dicarboxylic acid (2-oxoglutarate carrier-like protein). Given the important regulatory function of these enzymes, we conclude that pollen tubes respond to the loss of F-actin by inhibiting energy metabolism in pollen tubes. This represses respiration, leading to an inactive state, and suggests that the same mechanism may be at work in the repression of respiration during pollen germination and tube elongation.

Actin–ATP hydrolysis is a rate-limiting step in the actin treadmilling cycle (Didry *et al.*, 1998). Additionally, cellular depletion of ATP results in rapid actin depolymerization (Atkinson *et al.*, 2004; Jungbluth *et al.*, 1994) mediated by tyrosine-phosphorylation of actin (Jungbluth *et al.*, 1994), and in a reduction of actin gene expression (Brown and Davis, 2005). Engel *et al.* (1977) demonstrated that energy in the form of ATP contributed to actin polymerization, and that ATP-bound actin polymerized more quickly than ADP-bound actin, while the decline in cellular ATP associated with glucose depletion and oxidative phosphorylation resulted in disorganization of the actin cytoskeleton (Pendleton *et al.*, 2003). Our results suggest that ATP depletion promotes actin dephosphorylation (possibly via upregulated tyrosine phosphatase, see above) with increased levels of ADP-G-actin, which, in turn, promotes disruption of the actin cytoskeleton. Thus the downregulated enzymes identified provide a newly emerging link between energy metabolism and inhibition of actin cytoskeleton polymerization in plants.

Concluding remarks

Pollen germination, especially tube growth, in *P. meyeri* is strongly dependent on an intact actin cytoskeleton. The

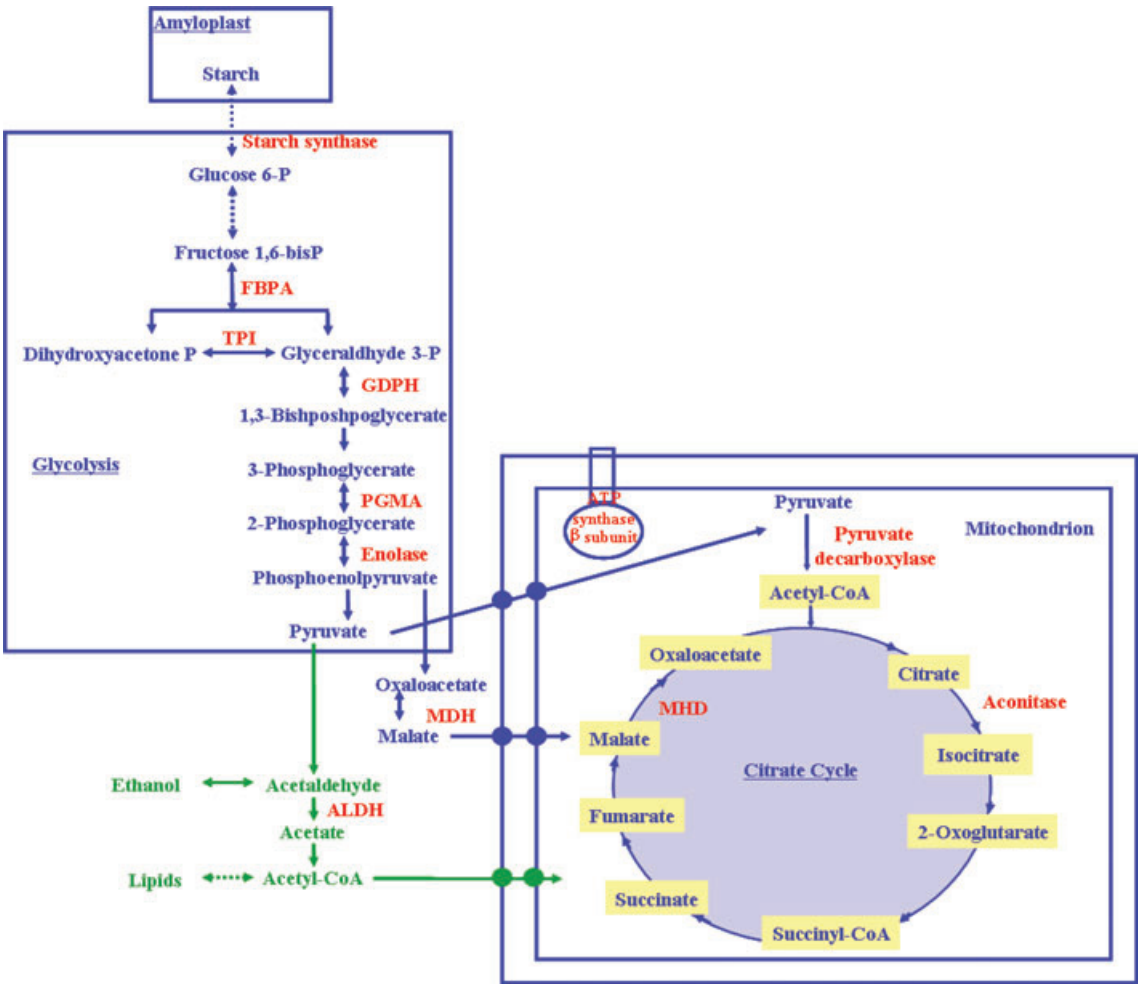

Figure 9. Graphical analysis of the putative function of several proteins involved in carbohydrate metabolism. Enzymes marked in red are identified as downregulated in actin-disrupted pollen tubes. They are involved in glycolysis, the citrate cycle, pyruvate dehydrogenase bypass (green) and oxidative phosphorylation.

proteomic analysis presented in this study has expanded our knowledge of the process by identifying dramatically changed proteins involved in crucial biological processes such as cell signalling, cell expansion and carbohydrate metabolism, as induced by selective F-actin disruption. Some of these proteins require further study. In addition to identifying and characterizing proteins important to pollen germination and tube development in *P. meyeri*, our results provide a general rationale for the role of the actin cytoskeleton in processes critical to pollen functionality. Our investigation also reveals the complex nature of molecular components affected by disruption of actin cytoskeleton. The factors that control pollen germination and tube growth are of considerable interest not only in understanding the metabolic processes involved in plant fertility and reproduction, but also for the development of molecular tools to manipulate pollen-tube growth for practical purposes and, last but not least, to understand plant polarity in general.

Experimental procedures

Chemicals

Latrunculin B, thiourea, CHAPS, SB3-10, ASB14, protease inhibitor cocktail, BSA, Folin-phenol reagent, TRITC-phalloidin, modified sequencing grade trypsin, ammonium carbonate and α-Cyano-4-hydroxycinnamic acid were from Sigma (St Louis, MO, USA). Urea, ampholine pH 3.5–10, idoacetamide, Destreak IPG strips and buffer were from Amersham Biosciences (Uppsala, Sweden). All other reagents were of highest purity grade and were purchased from Merck (Darmstadt, Germany).

Plant materials and treatments

Mature male cones of *P. meyeri* were collected manually in the Botanical Garden of the Institute of Botany, Chinese Academy of Sciences. The pollen grains were air-dried in the laboratory at room temperature for 48 h, then stored at −20°C until further use. For germination *in vitro*, pollen (approximately 100 mg) was cultured in 100-ml germination medium containing 12% sucrose, 0.02% H_3BO_3

and 0.02% $CaCl_2$. Latrunculin B was dissolved in DMSO as stock solution of 10 μM then transferred to the containers. The final concentration used in the experiment ranged from 1–150 nM. Moreover, the control was also cultured in the presence of DMSO: all working concentrations of DMSO were <1%, a level necessary to dissolve LATB and shown to have no effect on pollen germination and tube growth. The pollen germinated and pollen tubes elongated while cultured on a rotor (140 rpm) at 23°C.

Determination of pollen germination and pollen-tube growth

The percentage of germinated pollen grains and mean tube length were determined by counting at least 200 pollen grains under a light microscope. Pollen grains were considered to germinate when the pollen tube length was greater than the diameter of the pollen grain (Dafni, 2000). To measure the mean tube length, images of pollen tubes cultured in different media were taken at 4-h intervals after pollen germinated. All experiments were repeated three times and performed at room temperature.

Fluorescence labelling of F-actin

Samples were fixed in a freshly prepared solution of 4% paraformaldehyde in 50 mM Pipes buffer (pH 6.9) for 1 h. Following three washes in 50 mM Pipes buffer, the pollen tubes were incubated in enzyme solution containing 1% cellulase and 1% pectinase (in 50 mM Pipes buffer containing 0.1% protease inhibitor cocktail pH 6.9) at 37°C for 15 min. After three washes in 50 mM Pipes buffer, the pollen tubes were incubated in 1% Triton X-100 at room temperature for 40 min. After three washes, the samples were incubated in 0.2 nM phalloidin-TRITC in PBS (pH 6.9) buffer for 1 h in dark. They were mounted and images were collected in a Zeiss LSM 510 META laser scanning confocal microscope (Oberkochen, Germany). The fluorophore was excited with 515-nm line of Ar/Kr laser.

Electron microscopy

Pollen tubes were washed three times with 100 mM phosphate buffer (pH 7.2) and fixed for 2 h in 2.5% (v/v) glutaraldehyde in 100 mM phosphate buffer (pH 7.2). After washing in 100 mM phosphate buffer, samples were post-fixed in 1% osmium tetroxide for 2 h, dehydrated in an ethanol series, and finally embedded in Spurr's epoxy resin. Sections from at least 10 pollen tubes per treatment were cut using an LKB-V ultramicrotome, stained with 2% uranyl acetate (w/v) in 70% methanol (v/v) and 0.5% lead citrate, and observed under a JEM-1230 TEM (Jeol, Tokyo, Japan) at 80 kV.

Protein extraction

Cultured pollen tubes were filtrated from the culture medium then ground in a liquid nitrogen-cooled mortar, and the powder was suspended in a solution of 10% trichloroacetic acid in acetone containing 0.07% 2-mercaptoethanol. Proteins were precipitated for 2 h at −20°C. After centrifugation at 20 627 ***g*** for 10 min, protein pellets were rinsed with three volumes of ice-cold acetone containing 0.07% 2-mercaptoethanol at −20°C overnight. The supernatant was discarded, and the protein pellet air-dried and solubilized in a buffer containing 5 M urea, 2 M thiourea, 2% (w/v) CHAPS, 1% (w/v) SB3-10, 1% (w/v) ASB14, 2% (v/v) ampholine pH 3.5–10, 1% (v/v) protease inhibitor cocktail, and 50 mM dithiothreitol (DTT). Protein concentration was estimated using the Lowery method with a spectrophotometer (DU 640 Spectrophotometer; Beckman Coulter, Miami, FL, USA).

Two-dimensional electrophoresis (2-DE) and image analysis

2-DE was performed according to the Amersham 2-DE protocol. Prior to isoelectric focusing (IEF), each immobiline DryStrip (24 cm long, pH 3–10) was reswollen overnight in 450 ml rehydration solution (5 M urea, 2 M thiourea, 2% CHAPS, 1% SB3-10, 0.5% IPG buffer3-11, 1.2% Destreak and 0.002% bromophenol blue) at room temperature. The rehydration solution contained approximately 500 μg protein sample. IEF was carried out at 20°C on an IPGphor IEF system (Amersham Biosciences) with the following parameters: 500 V for 1 h, 1 kV for 1 h, followed by a step-by-step increase of voltage until 8 kV was reached for a total of 64 kVh. Before SDS–PAGE the strips were equilibrated for 15 min with a buffer containing 50 mM Tris–HCl (pH 8.8), 6 M urea, 30% glycerol, 2% SDS, 0.002% bromophenol blue and 1% DTT, followed for 15 min with the sample buffer but containing 2.5% idoacetamide instead of DTT. For 2-DE, the strips were loaded on 12.5% polyacrylamide gels and run at 40 mA per gel at 20°C until the tracking dye reached the bottom of the gel. All the experiments were repeated at least three times and remained highly reproductive. After electrophoresis, proteins were visualized by CBB staining.

CBB-stained gels were analysed with Image Master 2D PLATINUM 5.0 software (Amersham Biosciences). Using this software, spot detection, spot measurement, background subtraction and spot matching were performed. Following automatic spot detection, gel images were edited carefully. Prior to performing spot matching between gel images, one gel image was selected as the reference gel. After automatic matching, the unmatched spots of the member gels were added to the reference gel. The amount of a protein spot was expressed as the volume of that spot, defined as the sum of the intensities of all the pixels that make up the spot. In order to correct the variability due to CBB staining and to reflect quantitative variations in intensity of protein spots, spot volumes were normalized as a percentage of the total volume in all spots present in the gel. The resulting data from image analysis were transferred to the PLATINUM software for querying protein spots showing quantitative or qualitative variations. The apparent masses of the proteins detected on the two-dimensional gels were determined using marker proteins.

In-gel digestion

Protein spots were excised from the gels, destained with 50% (v/v) acetonitrile and 25 mM NH_4HCO_3, then incubated with 50 mM NH_4HCO_3 in 50% (v/v) methanol for 1 h at 40°C. Proteins were reduced with 10 mM DTT in 100 mM NH_4HCO_3 for 1 h at 60°C and alkylated with 40 mM iodoacetamide in 100 mM NH_4HCO_3 for 30 min at room temperature in the dark. The gels were dehydrated with SpeedVac concentrator (Thermo Savant, Holbrook, NY, USA), then rehydrated with 10 μl 25 mM NH_4HCO_3 containing 20 ng μl^{-1} trypsin at 37°C for 12–16 h. The peptide mixture was extracted with 0.1% trifluoroacetic acid (TFA) and 50% acetonitrile, finally the peptide solution was concentrated and stored at −20°C until use.

Protein identification by mass spectrometry

The trypsin-digested sample was desalted with ZipTip C18 (Millipore, Bedford, MA, USA) and mixed with the matrix

(α-cyano-4-hydroxycinnamic acid) dissolved in 0.5% TFA and 50% acetonitrile. The mixed solution was applied onto a stainless slide and then analysed in the Ettan MALDI-TOF mass spectrometer system (Amersham Biocsciences). Database searching was performed using the MASCOT search engine (available at http://www.matrixscience.com). To qualify as positive identification, the following typical criteria were used: database, NCBInr; taxonomy, *Viridiplantae* (green plants); one missed cleavage was allowed; peptide tolerance, 0.3; enzyme, trypsin; modifications (such as carbamidomethyl and oxidation) were used during matching. In addition, a significant MASCOT score and at least three independent peptides should match, and by combining observed MW and p*I* on the 2D gel, the identities of some proteins were finally determined.

In some cases a number of protein spots with uncertain identities were further selected and analysed using electrospray ionzation–tandem MS (ESI–MS/MS, Micromass, Manchester, UK).

Acknowledgements

This work was supported by the National Science Fund of China for Distinguished Young Scholars (30225005), and by grants from the EU Research Training Network TIPNET (project HPRN-CT-2002-00265), Brussels, Belgium; DAAD (Bonn, Germany, 323-PPP Slowakei), Deutsches Zentrum für Luft- und Raumfahrt (DLR, Bonn, Germany); and Grant Agencies APVT and Vega (grants APVT-51-002302 and 2031), Bratislava, Slovakia. We also thank Dr Wei Tang (Greenville, USA), Dr Mathew Benson (Canberra, Australia) and Dr Richard Turner (Ontario, Canada) for their patient correction of the draft of the manuscript.

References

Atkinson, S.J., Hosford, M.A. and Molitoris, B.A. (2004) Mechanism of actin polymerization in cellular ATP depletion. *J. Biol. Chem.* **279**, 5194–5199.

Baluška, F., Salaj, J., Mathur, J., Braun, M., Jasper, F., Šamaj, J., Chua, N.-H., Barlow, P.W. and Volkmann, D. (2000) Root hair formation: F-actin-dependent tip growth is initiated by local assembly of profilin-supported F-actin meshworks accumulated within expansin-enriched bulges. *Dev. Biol.* **227**, 618–632.

Baluška, F., Jasik, J., Edelmann, H.G., Salajova, T. and Volkmann, D. (2001) Latrunculin B-induced plant dwarfism: plant cell elongation is F-actin-dependent. *Dev. Biol.* **231**, 113–124.

Brown, R.C. and Davis, T.P. (2005) Hypoxia/aglycemia alters expression of occludin and actin in brain endothelial cells. *Biochem. Biophys. Res. Commun.* **327**, 1114–1123.

Bunney, T.D., van Walraven, H.S. and de Boer, A.H. (2001) 14–3-3 protein is a regulator of the mitochondrial and chloroplast ATP synthase. *Proc. Natl Acad. Sci. USA*, **98**, 4249–4254.

Callis, J. and Bedinger, P. (1994) Developmentally regulated loss of ubiquitin and ubiquitinated proteins during pollen maturation in maize. *Proc. Natl. Acad. Sci. USA*, **91**, 6074–6077.

Camacho, P. and Lechleiter, J.D. (1995) Calreticulin inhibits repetitive intracellular Ca^{2+} waves. *Cell*, **82**, 765–771.

Canovas, F., Gaudot, E.D., Rebecorbet, G., Jorrin, J., Mock, H.P. and Rossignol, M. (2004) Plant proteome analysis. *Proteomics*, **4**, 285–298.

Carbajo, R.J., Silvester, J.A., Runswick, M.J., Walker, J.E. and Neuhaus, D. (2004) Solution structure of subunit F(6) from the peripheral stalk region of ATP synthase from bovine heart. *J. Mol. Biol.* **342**, 593–603.

Chen, C., Wong, E.I., Vidali, L., Estavillo, A., Hepler, P.K., Wu, H.M. and Cheung, A.Y. (2002) The regulation of actin organization by actin-depolymerizating factor in elongation pollen tubes. *Plant Cell*, **14**, 2175–2190.

Clarke, S.R., Staiger, C.J., Gibbon, B.C. and Franklin-Tong, V.E. (1998) A potential signaling role for profilin in pollen of *Papaver rhoeas*. *Plant Cell*, **10**, 967–979.

Coué, M., Brenner, S.L., Spector, I. and Korn, E.D. (1987) Inhibition of actin polymerization by latrunculin A. *FEBS Lett.* **213**, 316–318.

Dafni, A. (2000) A new procedure to assess pollen viability. *Sex. Plant Reprod.* **12**, 241–244.

Dai, S., Li, L., Chen, T., Chong, K., Xue, Y. and Wang, T. (2006) Proteomic analyses of *Oryza sativa* mature pollen reveal novel proteins associated with pollen germination and tube growth. *Proteomics* **6**, 2504–2529.

Dhugga, K.S., Tiwari, S.C. and Ray, P.M. (1997) A reversibly glycosylated polypeptide (RGP 1) possibly involved in plant cell wall synthesis: purification, gene cloning, and trans-Golgi localization. *Proc. Natl Acad. Sci. USA*, **94**, 7679–7684.

Diaz-Camino, C., Conde, R., Ovsenek, N. and Villanueva, M.A. (2005) Actin expression is induced and three isoforms are differentially expressed during germination in *Zea mays*. *J. Exp. Bot.* **56**, 557–565.

Didry, D., Carlier, M.F. and Pantaloni, D. (1998) Synergy between actin depolymerizing factor/cofilin and profilin in increasing actin filament turnover. *J. Biol. Chem.* **273**, 25602–25611.

Engel, J., Fasold, H., Hulla, F.W. and Waechter, A. (1977) The polymerization reaction of muscle actin. *Mol. Cell. Biochem.* **18**, 3–13.

Faulkner, C.R., Blackman, L.M., Cordwell, S.J. and Overall, R.L. (2005) Proteomic identification of putative plasmodesmatal proteins from *Chara corallina*. *Proteomics*, **5**, 2866–2875.

Feijó, J.A., Costa, S.S., Prado, A.M., Becker, J. and Certal, A.C. (2004) Signalling by tips. *Curr. Opin. Plant Biol.* **7**, 589–598.

Fernando, D.D. (2005) Characterization of pollen tube development in eastern white pine (*Pinus strobus*) through proteomic analysis of differentially expressed proteins. *Proteomics*, **5**, 4917–4926.

Fernando, D.D., Owens, J.N., Yu, X.S. and Ekramoddoullah, A.K.M. (2001) RNA and protein synthesis during *in vitro* pollen germination and tube elongation in *Pinus monticola* and other conifers. *Sex. Plant Reprod.* **13**, 259–264.

Franke, W.W., Herth, W., VanDerWoude, W.J. and Morre, D.J. (1972) Tubular and filamentous structures in pollen tubes: possible involvement as guide elements in protoplasmic streaming and vectorial migration of secretory vesciles. *Planta*, **105**, 317–341.

Franklin-Tong, V.E. (1999) Signaling and the modulation of pollen tube growth. *Plant Cell*, **2**, 490–495.

Gallardo, K., Signor, C.L., Vandekerckhove, J., Thompson, R.D. and Burstin, J. (2003) Proteomics of *Medicago truncatula* seed development establishes related to reserve accumulation. *Plant Physiol.* **133**, 664–682.

Gibbon, B.C., Kovar, D.R. and Staiger, C.J. (1999) Latrunculin B has different effects on pollen germination and tube growth. *Plant Cell*, **11**, 2349–2363.

Gupta, R., Ting, J.T.L., Sokolov, L.N., Johnson, S.A. and Luan, S. (2002) A tumor suppressor homolog, AtPTEN1, is essential for pollen development in *Arabidopsis*. *Plant Cell*, **14**, 2495–2507.

Hao, H.Q., Li, Y.Q., Hu, Y.X. and Lin, J.X. (2005) Inhibition of RNA and protein synthesis in pollen tube development of *Pinus bungeana* by actinomycin D and cyloheximide. *New Phytol.* **165**, 721–730.

Hempel, J., Perozich, J., Romovacek, H., Hinich, A., Kuo, I. and Feingold, D.S. (1994) UDP-glucose dehydrogenase from bovine liver: primary structure and relationship to other dehydrogenases. *Protein Sci.* **3**, 1074–1080.

Hepler, P.K., Vidali, L. and Cheung, A.Y. (2001) Polarized cell growth in higher plants. *Annu. Rev. Cell Dev. Biol.* **17**, 159–187.

Holdaway-Clarke, T.L., Feijo, J.A., Hackett, G.R., Kunkel, J.G. and Hepler, P.K. (1997) Pollen tube growth and the intracellular cytosolic calcium gradient oscillate in phase while extracellular calcium influx is delayed. *Plant Cell*, **9**, 1999–2010.

Jin, J., Smith, F.D., Stark, C., Wells, C.D., Fawcett, J.P., Kulkarni, S., Metalnikov, P., O'Donnel, P., Taylor, P. and Pawson, T. (2004) Proteomic, functional, and domain-based analysis of *in vivo* 14-3-3 binding proteins involved in cytoskeletonal regulation and cellular organization. *Curr. Biol.* **14**, 1436–1450.

Jungbluth, A., von Arnim, V., Biegelmann, E., Humbel, B., Schweiger, A. and Gerisch, G. (1994) Strong increase in the tyrosine phosphorylation of actin upon inhibition of oxidative phosphorylation: correlation with reversible rearrangements in the actin skeleton of *Dicyostelium* cells. *J. Cell Sci.* **107**, 117–125.

Justus, C.D., Anderhag, P., Goins, J.L. and Lazzaro, M.D. (2004) Microtubules and microfilaments coordinate to direct a fountain streaming pattern in elongating conifer pollen tube tips. *Planta*, **219**, 103–109.

Kameyama, K., Kishi, Y., Yoshimura, M., Kanzawa, N., Sameshima, M. and Tsuchiya, T. (2000) Tyrosine phosphorylation in plant bending. *Nature*, **407**, 37.

Karamloo, F., Wangorsch, A., Hiroyuki, K., Davin, L.B., Haustein, D., Lewis, N.G. and Vieths, S. (2001) Phenylcoumaran benzylic ether and isoflavonoid reductases are a new class of cross-reactive allergens in birch pollen, fruits and vegetables. *Eur. J. Biochem.* **268**, 5310–5320.

Knorpp, C., Johansson, M. and Baird, A.M. (2003) Plant mitochondrial nucleoside diphosphate kinase is attached to the membrane through interaction with the adenine nucleoside translocator. *FEBS Lett.* **555**, 363–366.

Kwaaitaal, M.A.C.J., de Vries, S.C. and Russinova, E. (2005) *Arabidopsis thaliana* somatic embryogenesis receptor kinase 1 protein is present in sporophytic and gametophytic cells and undergoes endocytosis. *Protoplasma*, **226**, 55–65.

Lancelle, S.A. and Hepler, P.K. (1992) Ultrastructure of freeze substituted pollen tubes of *Lilium longiflorum*. *Protoplasma*, **167**, 215–230.

Lazzaro, M.D. (1998) The spermatogenous body cell of the conifer *Picea abies* (Norway spruce) contains actin microfilaments. *Protoplasma*, **201**, 194–201.

Lee, Y.R. and Liu, B. (2004) Cytoskeletal motors in Arabidopsis. Sixty-one kinesins and seventeen myosins. *Plant Physiol.* **136**, 3877–3883.

Meek, S.E., Lane, W.S. and Piwnica-Worms, H. (2004) Comprehensive proteomic analysis of interphase and mitotic 14-3-3-binding proteins. *J. Biol. Chem.* **279**, 32046–32054.

Murphy, A.S., Bandyopadhyay, A., Holstein, S.E. and Peer, W.A. (2005) Endocytotic cycling of PM proteins. *Annu. Rev. Plant Biol.* **56**, 221–251.

Parks, R.E.J. and Agarwal, R.P. (1973) Nucleoside diphosphokinases. *Enzyme*, **8**, 307–334.

Parton, R.M., Fischer-Parton, S., Watahiki, M.K. and Trewavas, A.J. (2001) Dynamics of the apical vesicle accumulation and the rate of growth are related in individual pollen tubes. *J. Cell Sci.* **114**, 2685–2695.

Pawson, T. and Nash, P. (2003) Assembly of cell regulatory systems through protein interaction domains. *Science*, **300**, 445–452.

Pendleton, A., Pope, B., Weeds, A. and Koffers, A. (2003) Latrunculin B or ATP depletion induces cofilin-dependent translocation of actin into nuclei of mast cells. *J. Biol. Chem.* **287**, 14394–14400.

Persson, S., Wyatt, S.E., Love, J., Thompson, W.F., Robertson, D. and Boss, W.F. (2001) The Ca^{2+} status of the endoplasmic reticulum is altered by induction of calreticulin expression in transgenic plants. *Plant Physiol.* **126**, 1092–1104.

Pierson, E.S., Miller, D.D., Callaham, D.A., Van, A.J., Hackett, G. and Helper, P.K. (1996) Tip-localized calcium entry fluctuates during pollen tube growth. *Dev. Biol.* **174**, 160–173.

Šamaj, J., Ovecka, M., Hlavacka, A. *et al.* (2002) Involvement of the mitogen-activated protein kinase SIMK in regulation of root hair tip growth. *EMBO J.* **21**, 3296–3306.

Šamaj, J., Baluška, F., Voigt, B., Schlicht, M., Volkmann, D. and Menzel, D. (2004) Endocytosis, actin cytoskeleton and signalling. *Plant Physiol.* **135**, 1150–1161.

Šamaj, J., Read, N.D., Volkmann, D., Menzel, D. and Baluška, F. (2005) The endocytic network in plants. *Trends Cell Biol.* **15**, 425–433.

Sehnke, P.C., Chung, H.J., Wu, K. and Ferl, R.J. (2001) Regulation of starch accumulation by granule-associated plant 14-3-3 proteins. *Proc. Natl Acad. Sci. USA*, **98**, 765–770.

Shah, K., Vervoort, J. and de Vries, S.C. (2001) Role of threonines in the AtSERK1 activation loop in phosphorylation. *J. Biol. Chem.* **276**, 41263–41269.

Shen, S.H., Jing, Y.X. and Kuang, T.Y. (2003) Proteomics approach to identify wound-response related proteins from rice leaf sheath. *Proteomics*, **3**, 527–535.

Sherrier, D.J. and VandenBosch, K.A. (1994) Secretion of cell wall polysaccharides in *Vicia* root hairs. *Plant J.* **5**, 185–195.

Spector, I., Shochet, N.R., Kashman, Y. and Groweiss, A. (1983) Latrunculins: novel marine toxins that disrupt microfilament organization in cultured cells. *Science*, **219**, 493–495.

Staiger, C.J. (2000) Signaling to the actin cytoskeleton in plants. *Annu. Rev. Plant Physiol. Plant Mol. Biol.* **51**, 257–288.

Staiger, C.J. and Hussey, P.J. (2004) Actin and actin-modulating proteins. In *The Plant Cytoskeleton in Cell Differentiation and Development* (Hussey, P., ed.). Oxford, UK: Blackwell, pp. 1–49.

Staiger, C.J., Baluška, F., Volkmann, D. and Barlow, P.W. (eds) (2000) *Actin: A Dynamic Framework for Multiple Plant Cell Functions*. Dordrecht, the Netherlands: Kluwer Academic.

Tadege, M., Dupuis, I. and Kuhlemeier, C. (1999) Ethanolic fermentation: new functions for an old pathway. *Trends Plant Sci.* **4**, 320–325.

Vidali, L., Sylvester, T.M. and Hepler, P.K. (2001) Actin polymerization is essential for pollen tube growth. *Mol. Biol. Cell*, **12**, 2534–2545.

Voigt, B., Timmers, T., Šamaj, J. *et al.* (2005) Actin-based motility of endosomes is linked to the polar tip growth of root hairs. *Eur. J. Cell Biol.*, **84**, 609–621.

Volkmann, D. and Baluška, F. (1999) The actin cytoskeleton in plants: from transport networks to signaling networks. *Microsc. Res. Tech.* **47**, 135–154.

Walter, M.M., Kathryn, R.A. and Paul, J.M. (2000) Latrunculin alters the actin–monomer subunit interface to prevent polymerization. *Nat. Cell Biol.* **2**, 376–378.

Wang, Q., Kong, L., Hao, H., Wang, X., Lin, J., Šamaj, J. and Baluška, F. (2005) Effects of Brefeldin A on pollen germination and tube growth: antagonistic effects on endocytosis and secretion. *Plant Physiol.* **139**, 1692–1703.

Wilkins, M.R., Sanchez, J.C., Gooley, A.A., Appel, R.D., Humphery-Smith, I., Hochstrasser, D.F. and Williams, K.L. (1996) Progress

with proteome projects: why all proteins expressed by a genome should be identified and how to do it. *Biotechnol. Genet. Eng. Rev.* **13**, 19–50.

Wilson, C., Voronin, V., Touraev, A., Vicente, O. and Herberle-Bors, E. (1997) A developmentally regulated MAP kinase activated by hydration in tobacco pollen. *Plant Cell*, **9**, 2093–2100.

Zhang, Q. and Salter, R.D. (1998) Distinct patterns of folding and interactions with calnexin and calreticulin in human class I MHC proteins with altered *N*-glycosylation. *J. Immunol.* **160**, 831–837.

